FINITE ELEMENT MODELLING OF CONCRETE FILLED STEEL TUBULAR COLUMNS

A
Dissertation
Submitted in partial fulfilment of the requirement for the award of degree of

MASTER OF ENGINEERING
IN
STRUCTURAL ENGINEERING

Submitted

By

Arvind Thakur
(Roll No. 801222001)

Under Supervision of

Dr. Naveen Kwatra
Head and Associate Professor
Civil Engineering Department

CIVIL ENGINEERING DEPARTMENT
THAPAR UNIVERSITY
PATIALA-147004, PUNJAB

July 2014

CERTIFICATE

I, "Arvind Thakur", hereby certify that the work which is being presented in this thesis report entitled **"Finite Element Modelling of Concrete Filled Steel Tubular Columns"** by me in partial fulfilment of the requirements for the award of degree of **Master of Engineering (Structural Engineering)** in **Civil Engineering** from **Thapar University, Patiala,** is an authentic record of my own work carried out under the supervision of **Dr. Naveen Kwatra, Associate Professor and Head, Department of Civil Engineering**, Thapar University, Patiala.

The matter embodied in this thesis has not been submitted in any other University / Institute for the award of any other degree.

Arvind Thakur

Date: 18/7/2014

(ARVIND THAKUR)
Reg. No. 801222001

This is to certify that the above statement made by the student concerned is correct to the best of my knowledge and belief.

Date: 18/7/2014

(Dr. NAVEEN KWATRA)
Associate Professor and Head,
Civil Engineering Department,
Thapar University,
Patiala (Punjab)

Countersigned by

(Dr. NAVEEN KWATRA)
Associate Professor and Head,
Civil Engineering Department,
Thapar University,
Patiala (Punjab)

(Dr. S.K. MOHAPATRA)
Dean of Academic Affairs,
Thapar University,
Patiala (Punjab)

ACKNOWLEDGEMENT

With deep sense of gratitude I would like to express deepest appreciation and sincere thanks to my advisor, **Dr. Naveen Kwatra,** who has the attitude and the substance of a genius.

Dr. Naveen Kwatra continually and convincingly conveyed a spirit of adventure in regard to research and an excitement in regard to teaching. Without his guidance and persistent help this dissertation would not have been possible.

The opportunity, support, exposure and atmosphere provided by the Thapar University, Patiala, to carry out my studies is highly appreciated.

A special debt of gratitude is owed to the authors whose works I have consulted and quoted in this work.

Last but not least, I am forever grateful to my parents for their unconditional support and best wishes.

ARVIND THAKUR

ABSTRACT

To model the complex behaviour of concrete filled steel tubular columns (CFST) analytically in its non-linear zone is difficult. This has led engineers in the past to rely heavily on empirical formulas which were derived from numerous experiments for the design of concrete filled steel tubular columns.

The Finite Element method makes it possible to take into account non-linear response. The FE method is an analytical tool which is able to model composite structures and is able to calculate the non-linear behaviour of the structural members. For structural design and assessment of composite structures, the non-linear finite element (FE) analysis has become an important tool. The method can be used to study the behaviour of reinforced, pre-stressed concrete structures and concrete filled steel tubes i.e. composite structures including both force and stress redistribution.

The Finite Element method allows complex analysis of the nonlinear response of concrete filled steel tubular column to be carried out in a routine fashion. FEM helps in the investigation of the behaviour of the structure under different loading conditions and its load deflection behaviour.

In the present study, the non-linear response of concrete filled steel tubular column using FE Modelling under the axial loading has been carried out with the intention to investigate the relative importance of several factors in the non-linear finite element analysis of concrete filled steel tubular columns. These include the variation in load displacement graph and the crack patterns of concrete filled steel tubular columns. Finally results from FEM compared with experimental results and comparative study shows the behaviour of concrete filled steel tubular columns under axial loading.

TABLE OF CONTENTS

CONTENTS

LIST OF FIGURES

LIST OF TABLES

CHAPTER 1 INTRODUCTION

1.1 GENERAL

Concrete filled steel tubes (CFST) are composite structures consisting of a steel tube infilled with concrete. In present international practice, CFST columns are used in the primary lateral resistance systems of both braced and unbraced building structures. CFSTs may be operated for retrofitting purposes for strengthening concrete columns in earthquake prone areas.

Concrete filled steel tubes are generally used in

- Beams.
- Columns.
- Piers and caissons for deep foundations.

Concrete filled steel tubular columns have been utilized in dwelling houses, tall buildings and many types of arch bridges. Steel hollow sections used as reinforcement in this composite structure. CFST columns has established an appropriate loading capacity, ductility and energy absorption capacity. The steel tube functions as the formwork for casting the concrete and hence, construction cost is reduced. There is no other reinforcement and the tube acts as longitudinal and lateral reinforcement for the concrete core. An evaluation of available experimental studies shows that the main parameters influencing the behaviour and strength of concrete filled steel tubular columns are slenderness, the diameter to wall thickness (D/t) ratio and the initial geometry of the column. The mechanical parameters, such as the strength of the steel and concrete are also the main parameters. [6]

In innovative CFST structures, silica fume which is supplementary cementitious material, are usually added into the concrete mix to obtain higher strength and better performance of the structure. CFST columns having addition of silica with concrete in this way are known as high strength concrete filled steel tubular columns. For high strength concrete filled steel tubular columns, there is a composite action between these two essential elements which contributes the concrete to prevent inward buckling of wall of steel tube. Steel tube in concrete filled steel tubular columns acts as reinforcement for the structure. This steel tube also provides confining pressure to the

concrete which results in reducing the brittleness high strength concrete core and improves the mechanical properties of the structure. [17]

Concrete filled steel tubes also used fiber reinforced polymers as the composite material and is known as concrete filled fiber reinforced polymer tubes. There composite action results in resisting development of crack and gives better ductility. Fiber reinforced concrete as composite material consist of concrete reinforced by random placement of short, discontinuous and discrete fibers of specified geometry. Fiber reinforced polymer is more economically superior to the traditional techniques in many conditions. Fiber reinforced polymer is lighter, more durable, fire resistant and higher strength to weight ratio as compared to the traditional materials like steel. [18]

Concrete filled steel stub columns exhibits higher strength and fire resistant property over bare steel columns, larger stiffness and ductility. In previous, a large number of studies had been carried out to examine the realistic behaviour of concrete-filled steel tube (CFST) columns under post fire conditions. Structural members will experience several phases like the initial loading, the heating phase with the development of fire, and the cooling phase when subjected to fire. If the member survives after the fire, its residual strength needs to be assessed to check its appropriateness for frequent use. So, finite element analysis (FEA) models are prepared for studying the behaviour of concrete filled CHS (circular hollow section) and SHS (square hollow section) stub columns under the various combinations of thermal and mechanical loading. [23]

1.2 HISTORY

Pre 1960's

Revolution and requirement have been dynamism for the structural design throughout the history. As early in 1930's, the former SOVIET UNION constructed a 101m bridge by using concrete filled steel tubes. Nominal research and experience using concrete filled steel tubes formed anxiety of using CFST.

1960's - 1980's

In 1961 Kato Naka wrote the first technical journal on CFST in Japan which described circular CFST compression member used in power transmission tower. This technical paper study on the subject leading to addition of the architectural institute of the Japan

(AIJ) standard for concrete and circular steel tubes as the composite structures, published in 1967. China and Japan made investments in research for setting the foundation of CFST.

1980's – 1990's

In 1980, revision of standards was carried out by Architectural Institute of Japan (AIJ) to include square steel tubes and their limitations. Japan ministry of construction competition was held on 1985 for the construction of urban apartment houses in 21st century which leads to advanced application of the CFSTs. Five contractors and a steel manufacturer won the competition. These five contractors and that steel manufacturer along with the Building research institute (BRI) of the ministry of the construction of the Japan stared a five year experimental research project called New Urban Housing Project. In 1993, another five year research project on the hybrid and composite structures as the fifth phase of the U.S. – Japan Collaboration Earthquake Research Program and the investigation the CFST column system was included in the program research findings obtained from this project made the present design recommendations for the CFST column system.

1.3 TYPES OF CFST

Concrete filled steel tubes is designed on the basis of their application. It may be square, hexagonal and circular depends upon design and use of their application. Concrete filled steel tubes are divided into two types according to the form of the concrete core. These two types are solid and hollow concrete core CFSTs. In Fig.1.1 some shapes of CFST are shown which indicates these both types. Solid concrete core is made by placing the plain concrete in the steel tube and compaction is done by vibration. Hollow concrete filled steel tubes is made by spinning method. The method of insertion of the wet concrete in the rotational mould is known as spinning method. Where wet concrete is compacted by vibration using centrifugation due to rotation of the mould.

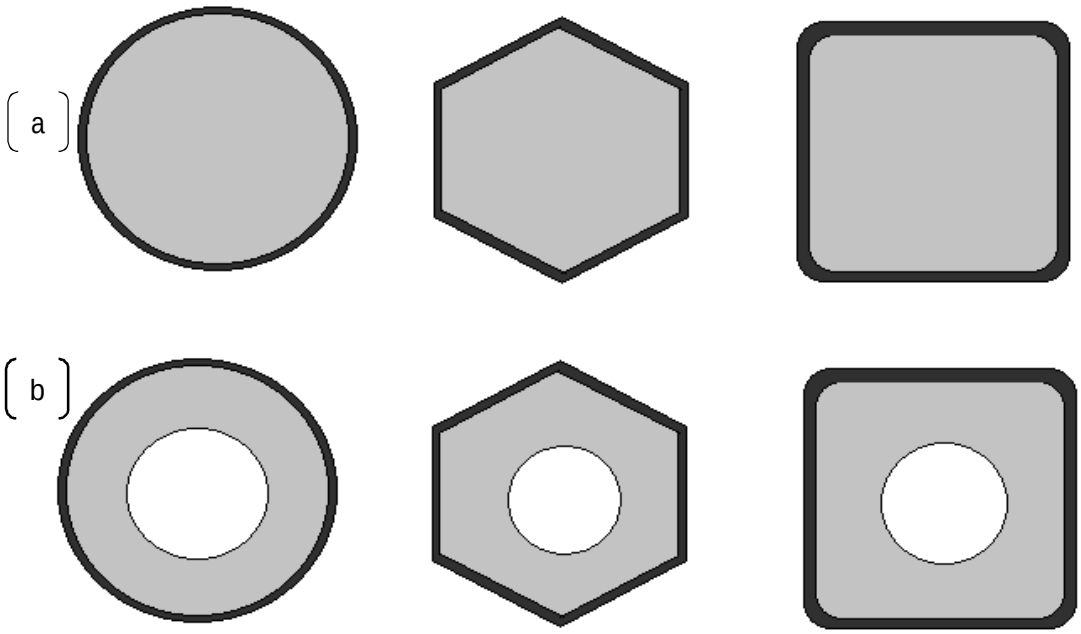

Fig.1.1 Cross-sections of solid and hollow CFST composite columns.

1.4 BEHAVIOUR OF CFST

Many previous studies have shown that square concrete filled steel tubes is not as good compare to circular concrete filled steel tubes. This is due to the confining pressure acts in concrete core by square steel tube is less and that's why local buckling more likely to occur. The structural behaviour of the concrete filled steel tube is affected by the Poisson's ratio of both steel and concrete. At the initial stage of loading, Poisson's ratio of the concrete is lower than that of steel. Hence the steel tube does not contribute confining effect to the concrete. When the longitudinal strain increases, lateral expansion of the concrete gradually becomes greater than the expansion of the steel tube. At this stage of loading, steel tube becomes biaxially stressed and concrete core becomes triaxially stressed. So due to the biaxial stress in the steel tube, the steel tube cannot sustain normal yield stress and hence transfer the load from tube to core. The load transfer mechanism is same for both circular and square concrete filled steel tubes.

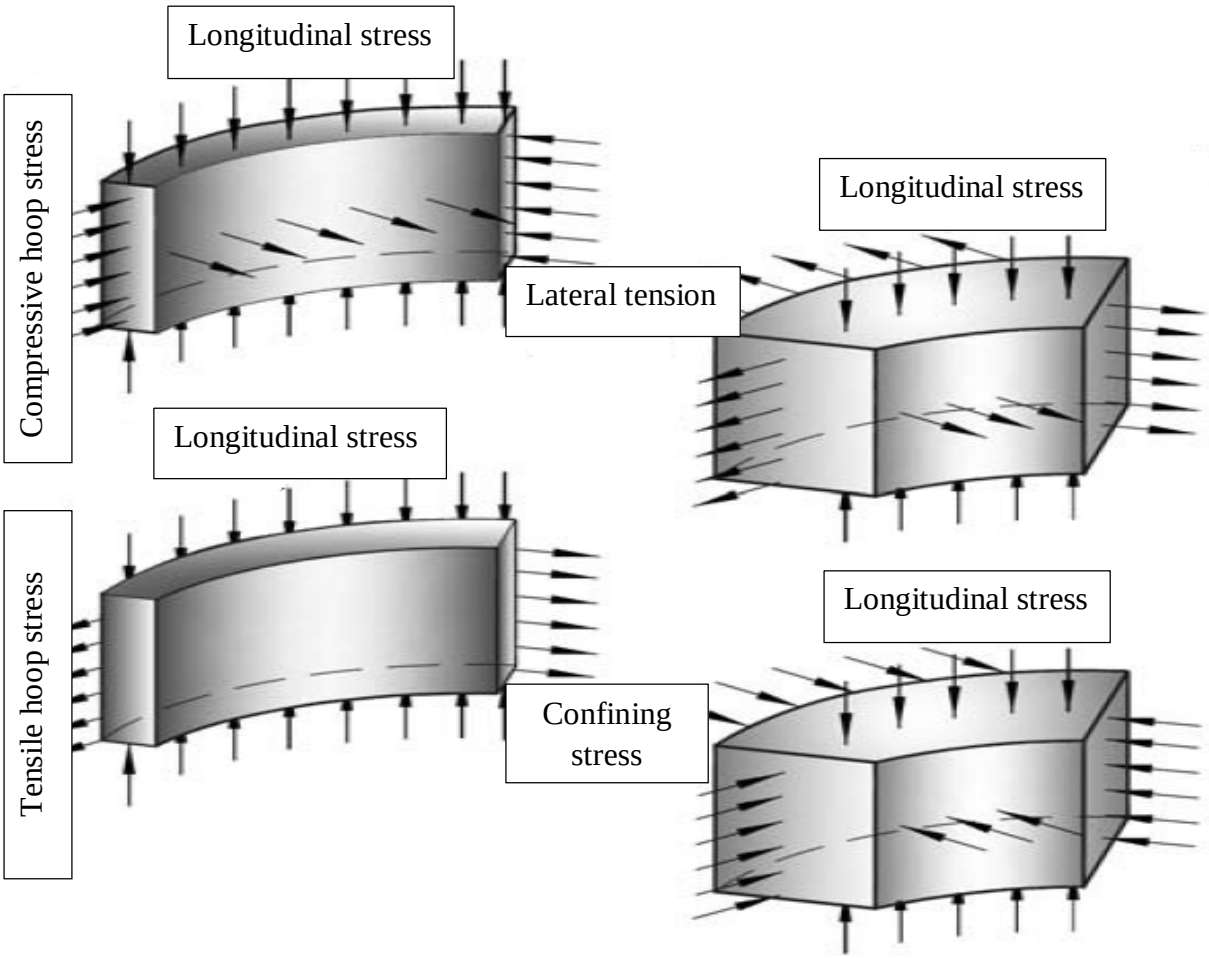

Fig.1.2 Stress condition in steel tube and concrete core at different stages of loading.

1.5 ADVANTAGES OF CFST

The CFST structural member has many distinctive advantages above equivalent steel, reinforced concrete and steel-reinforced concrete member. Hence the advantages are as follows.

(1) The steel at the outer perimeter in CFST serves most effectively in tension and also resists bending moment.

(2) The stiffness of the CFST is greatly improved because the steel which has higher modulus of elasticity than the concrete, is located farthest from the centroid contributes large moment of inertia.

(3) The concrete forms an ideal core to bear the compressive loading in typical applications, and it suspend and often avoids local buckling of the steel, particularly in rectangular CFSTs.

(4) Steel tube confines concrete core which increases the compressive strength of circular CFSTs and also increases ductility of rectangular CFSTs. Hence, it is most beneficial to use CFSTs for the columns subjected to the large compressive loading.

(5) In reinforced concrete columns having transverse reinforcement, it minimizes the congestion of reinforcement and also minimizes the spalling of concrete, especially for seismic design.

(6) When thin walled steel tubes and high strength concrete are used together, more brittle nature of high strength concrete is partly mitigated by the confinement offered by steel tube. Due to support offered by the concrete, local buckling of thin steel tube is delayed.

(7) The tube acts as formwork in construction of concrete filled steel tubes, which decreases labour and material costs.

(8) Smaller column sizes may be used in high strength applications, increasing the amount of usable floor space in office buildings. The smaller and lighter framework places less of a load on the foundation, reduces the costs again.

(9) CFST has good fire resistance due to concrete present in it. So that fireproof material can be reduced or omitted.

(10) CFST performs ecology purpose also. By reusing the steel pipes and use of recycled aggregates with high quality concrete, environmental burden can be reduced by omitting the formwork.

1.6 IMPORTANCE OF FINITE ELEMENT MODELLING

To model the composite behaviour of concrete filled steel tubular columns analytically in its non-linear zone is difficult. This has led the engineers in the past to rely seriously

on empirical formulas which were derived from several experiments for the design of concrete filled steel tubular columns.

The Finite Element Method makes it possible to take into account non-linear response. The Finite Element Method is an analytical tool which is able to model concrete filled steel tubular columns and is able to calculate the non-linear behaviour of the structural members. Finite element method is the dominant discretization technique in structure analysis. The basic concept of the Finite Element Method is the subdivision of the mathematical model into disjoint (non-overlapping) components of simple geometry called finite elements or elements for short. The response of each element is expressed in terms of a finite number of degrees of freedom characterized as the value of an unknown function, or functions, at a set of nodal points. The method can be used to study the behaviour of concrete filled steel tubular column structures including both force and stress redistribution. FEM is useful for obtaining the load deflection behaviour and its crack patterns in various loading conditions. [5]

A typical finite element analysis on a software system requires the following information.

1. Nodal point spatial locations (geometry).
2. Elements connecting the nodal points.
3. Mass properties.
4. Boundary conditions or restraints.
5. Loading or forcing function details.
6. Analysis options.

With the improvement of digital computers and powerful methods of analysis, such as the finite element method, many efforts to develop analytical solutions which would obviate the need for experiments have been undertaken by investigators. The finite element method has thus become a powerful computational tool, which allows complex analysis of the nonlinear response of concrete filled steel tubular columns to be carried out in a simple way.

1.7 OBJECTIVES

In the present study, the non-linear response of concrete filled steel tubular columns using FE Modelling under the axial loading has been carried out with the purpose to examine the relative importance of several factors in the non-linear finite element analysis of concrete filled steel tubular columns. This includes the variation in load deformation graph and the crack patterns on the analytical results and the effect of the non-linear behaviour of concrete and steel on the response of deformed CFST column.

The main objectives of the present study are as follows.

1. To study the response and loading capacity of concrete filled steel tubular columns using non-linear finite element analysis.

2. To model the concrete filled steel tubular columns using finite element software.

3. To compare the results of deformed concrete filled steel tubular column with the experimental results of previous research paper.

1.8 SCOPE OF THE WORK

In the present study of FE modelling of the control concrete filled steel tubular columns under the axial loading has been analyzed using ATENA software and the results so obtained have been compared with available experimental results from Uy et al. (2009).

Concrete filled steel tubular column is analyzed using ATENA software up to the failure and the load deformation curves are plotted. The control concrete filled steel tubular columns has been analyzed and results have been compared with the experimental results. Comparisons are made by the load deflection curves and values. Deflection of the columns at every load step are also studied.

1.9 ORGANIZATION OF THE THESIS

The thesis is organized in the following way:

Chapter 1: Introduces the topic of thesis in brief.

Chapter 2: Discusses the literature review i.e. the work done by various researchers in the field of concrete filled steel tubular columns under axial loading.

Chapter 3: Deals with the details of the structure modelled in ATENA in its first part. Second part comprises of FEM modelling, theory related to the ATENA, material modelling and analytical programming procedure steps involved in modelling of the control CFST column. It also deals with the description of the material behaviour of concrete and steel tube.

Chapter 4: The results from the analysis, comparison between the analytical and the experimental results of the CFST column, all are discussed in.

Chapter 5: Finally, salient conclusions and recommendations of the present study are given in this chapter followed by the references.

CHAPTER 2 LITERATURE REVIEW

2.1 GENERAL

It would be difficult to present the detailed review of the literature related to FE modelling of concrete filled steel tubular columns so a brief review of previous studies on the application of the finite element method and experiment analysis of concrete filled steel tubular columns is presented in this chapter.

This literature review focuses on recent contributions related to concrete filled steel tubular columns, materials used for concrete filled steel tubular columns and past efforts most closely related to the needs of the present work.

2.2 FINITE ELEMENT MODELLING OF CONCRETE FILLED STEEL TUBULAR COLUMNS

Schneider, (1998) investigated the behaviour of short concrete filled steel tube columns concentrically loaded in compression to failure. Experimental and analytical study was carried out to find the behaviour of concrete filled steel tube columns. Fourteen specimens were tested to investigate the effect of the steel tube shape and wall thickness on the ultimate strength of the composite column. Length of all columns were same. Depth-to-tube wall thickness ratios between $17 < D/t < 50$, and the length-to-tube depth ratios of $4 < L/D < 5$ were investigated. Ultimate strength results were compared to current specifications governing the design of concrete-filled steel tube columns. Nonlinear finite-element models were developed by using ABAQUS software and verified these analytical results with experimental results. The concrete core of the concrete filled steel tube columns was modelled using 20-node brick elements, with three translation degrees of freedom at each node and steel tube was modelled using an 8-node shell element, with five degrees of freedom at each node. The three-dimensional concrete material model available in ABAQUS was developed to simulate conditions with uniaxial strain and relatively low confining pressure. The analytical models were further used to investigate the adequacy of design specifications. Experimental results suggest that circular tubes offer substantial post-yield strength and stiffness, not available in most square or rectangular cross sections. Also observed by these results was that current

design specifications were adequate to predict the yield load under most conditions for a variety of structural shapes. [21]

Hu et al., (2005) presented the paper on finite element analysis of CFST columns subjected to an axial compressive force and bending moment in combination. Proper material constitutive models for concrete filled steel tube (CFST) columns subjected to an axial compressive force and bending moment in combination are proposed and verified in this paper by using the nonlinear finite element program ABAQUS compared against experimental data. In the numerical analysis, the cross sections of the CFST columns are categorized into three groups, i.e., ones with circular sections, ones with square sections, and ones with square sections stiffened with reinforcing ties. In the analysis, the Poisson's ratio μ_s and the elastic modulus E_S of the steel tube are assumed to be 0.3 and 200 GPa, respectively. In this study, the Poisson's ratio of concrete is assumed to be 0.2. The uniaxial behaviour of the steel tube is similar to that of the reinforcing tie and thus can be simulated by an elastic–perfectly plastic model. It is shown that the steel tubes can provide a good confining effect on the concrete core when the axial compressive force is large. The confining effect of a square CFST stiffened by reinforcing ties is stronger than that of the same square CFST without stiffening ties but weaker than that of a circular CFST. However, when the spacing of reinforcing ties is small, a CFST with a square section might possibly achieve the same confining effect as one with a circular section. [14]

Gupta et al., (2007) presented experimental and computational study on the behaviour of circular concentrically loaded concrete filled steel tube columns till failure. Eighty-one specimens were tested to investigate the effect of diameter and D/t ratio of a steel tube on the load carrying capacity of the concrete filled tubular columns. The effect of the grade of concrete and volume of flyash in concrete was also investigated. The effect of these parameters on the confinement of the concrete core was also studied. Diameter to wall thickness ratio between $25 < D/t < 39$, and the length to tube diameter ratio of $3 < L/D < 8$ was investigated. Strength results of Concrete Filled Tubular columns were compared with the corresponding findings of the available literature. Also a nonlinear finite element model was developed to study the load carrying mechanism of CFSTs using the Finite Element software ANSYS. This model was validated by comparison of the experimental and computational results of load–deformation curves and their

corresponding modes of collapse. The displacement at the yield point is found to be 2–3 mm (about 20%–30%) less in the case of the computational graphs when compared with the experimental one for all types of specimens From the experimental and computational study it was found that for both modes of collapse of concrete filled tubular columns at a given deflection the load carrying capacity decreases with the increase in % volume of flyash up to 20% but it again increases at 25% flyash volume in concrete. [13]

Uy et al., (2009) studied the behaviour of slender square concrete filled stainless steel columns subjected to the axial load. Due to its excellent corrosion resistance, decorative qualities, ease of maintenance and fire resistance, the past few decades have seen the accelerating interest in the use of stainless steel in construction throughout the world. A total of 6 square concrete filled steel tubular columns were tested under axial loading to evaluate the influence of global slenderness. Two concrete grades were used having concrete cylindrical strength of 36.3 MPa and 75.4 MPa and slenderness ratio limits from 15.2 to 87.7. Several existing design codes, including the Australian design code AS 5100 (2004), American code AISC (2005), Chinese code DBJ 13-51-2003 (2003) and Eurocode 4 (2004), are used to predict the column strength and are compared with the test results. This is helpful in evaluating the applicability of the current codes in calculating the strength of slender square concrete filled stainless steel tubular columns. It was found that the larger the slenderness ratio the smaller the peak load is. As stainless steel tube was used to compare the results between carbon steel and stainless steel. As there was no obvious difference between carbon steel and stainless steel tubes in terms of test observations and failure modes. Composite action between steel tube and concrete core still exists for slender concrete filled stainless steel columns, but this action decreases with increasing slenderness ratio. Slenderness reduction factors should be applied in designing slender concrete filled stainless steel columns. [25]

Ghannam et al., (2010) conducted the tests on steel columns filled with normal concrete and lightweight concrete were carried out to investigate the actual behaviour and the load carrying capacity of such columns. Eight full scale rectangular cross-section columns filled with lightweight aggregate concrete and normal weight aggregate concrete, four specimens each, were tested under axial loads for comparison purposes. Sections filled with lightweight aggregate concrete failed due to local as well as overall buckling, and they supported more than 92% of the squash load. Sections filled with normal weight

aggregate concrete failed due to overall buckling at mid height, and they supported more than 87% of the squash load. It can obviously be seen that columns with lightweight aggregate concrete filled steel tubular support similar loads as columns filled with normal weight aggregate concrete. On the other hand, the weight of the column with lightweight concrete was 30% less than that of the column with normal concrete of the same cross-section. It can obviously be seen that columns with lightweight aggregate concrete filled steel tubular support similar loads as columns filled with normal weight aggregate concrete. On the other hand, the weight of the column with lightweight concrete was 30% less than that of the column with normal concrete of the same cross-section. Hence the results showed that using lightweight concrete filling instead of normal concrete filling will reduce the weight of columns. At the same time, a high load carrying capacity is achieved. [12]

Kwasniewski et al., (2011) presented the numerical part of the research program on concrete-filled steel columns. Nonlinear, three dimensional FE analysis of axial compression, was conducted using the finite element program ABAQUS. Four steel tube columns were taken in which two were without concrete and other two were filled with concrete. The numerical results were validated through comparison with experimental data in terms of ultimate loading and deformation modes. To avoid numerical problems the inelastic material response should be approximated by curves with a limited number of points. The magnitude of the yield stress is critical for ultimate load estimation. The effect of residual stresses due to welding of the side plates was not taken into account in the presented research. Imperfections in the form of loading eccentricity do not reduce the ultimate load significantly but can change the deformation pattern. This explains the variation of deformation obtained in the experiment. The effect of imperfections highlights the importance of precise measurements before testing to evaluate the actual geometrical imperfections. Modelling related problems such as the definition of boundary conditions, imperfections, concrete-steel interaction, material representation and others are investigated using a comprehensive parametric study. The developed FE models will be used for an enhanced interpretation of experiments and for the predictive study of cases not included in the experimental testing. [16]

Gajalakshmi et al., (2011) investigated the behaviour of concrete filled steel columns. In the this paper, experimental results of concrete–filled steel columns and polymer

modified concrete filled steel columns under axial load combined with lateral cyclic loading were reported. Circular CFST model columns with steel tube diameter-thickness ratio (D/t) of 57 were tested to failure. This ratio satisfies the limitations specified by various codes. The yield stress and ultimate stress of steel section were found to be 270 N/mm^2 and 410 N/mm^2 respectively and the percentage elongation was 13% and modulus of elasticity was 2.05×10^5 N/mm^2. The design mix of 1: 2.09: 2.25 with a w/c ratio of 0.49, using 12.5mm size (max.) coarse aggregate and 2.36mm (max.) size fine aggregate was used as per ACI committee 211.1.1991 recommendations. The PCC (Portland cement concrete) and PMC (polymer modified concrete) for the composite columns were mixed in two separate batches. To assess the compressive strength, cubes of size 150 mm x 150 mm x 150 mm and cylinders of size 300mm x 150mm were cast. It was found that Polymer modified concrete filled steel columns fail in a ductile manner and exhibit plump hysteretic loops with a slight pinching effect under the combination of axial load and lateral cyclic load. Polymer modified concrete filled columns exhibit high ductility with moderate axial strength increase, an attribute that has become of great necessity in currently emphasized ductility oriented seismic design. [11]

Kvocak et al., (2012) presented the preparation and execution of an experimental programme focusing on the verification of rectangular composite members subjected to compression. A total of 12 simple laboratory specimens were designed for the experimental research programme. The overall length of the experimental columns was 2.7m, whereas the steel casing of the columns was 2.6m long. The steel section of the columns was made of thin-walled welded sections 2mm thick. The load intensity was opted to capture all examined parameters as authentically as possible and the load incrementally increased by 15.4 KN. The examined specimen was unloaded once, from 154 KN to 77 KN. The test was completed when the specimen was not capable of sustaining greater load. At this stage excessive deflections occurred in the examined specimens with no further increase in load. Emphasis was placed on both global stability of the column and the local stability of the thin column plates. Upon the completion of all experiments, the members will be modelled using the numerical computational tools such as ANSYS and ABAQUS software packages whose results will be compared with the experimentally attained values. Based on such extensive findings conclusions and recommendations for the general public and professionals will be made. [15]

Dundu, (2012) investigated the behaviour of 24 concrete filled steel tubes (CFST) columns, loaded eccentrically in compression to failure. Parameters in the tests include length, diameter, strength of the steel tubes and the strength of the concrete. These tests were divided into two series i.e. Series-1 and Series-2. Each Series has 12 specimens. Diameters 114.3mm, 127.0mm and 139.7mm of columns in series-1 were used. Diameters 152.4mm, 165.10mm and 193.70mm of columns in series-2 were used. Length of 1m, 1.5m, 2m and 2.5m were used. Concrete mix is designed for compressive cube strength (f_{cu}) at 28 days of approximately 40MPa for series-1 and 30MPa for series-2. As the length of the composite column increases, the load carrying capacity decreases. Bearing capacities of the composite columns decreases with the increase of the slenderness ratio. Beneficial effects of confinement decrease as the column length increases. Confinement effects are significant for circular short columns subjected to concentric loading. In slender columns, confinement effects are negligible since the lateral deflection prior to failure increases the bending moment and reduce the mean compressive strain in the concrete. All columns behaved in a fairly ductile manner. Ductility was more pronounced in short than slender columns. [8]

Patil, (2012) investigated the behaviour of Concrete filled steel tubular column on the compressive response due to axial loads. Three-dimensional nonlinear finite element models are developed to study the force transfer between steel tube and concrete core. The nonlinear finite element program ABAQUS 6.8 is used. The interaction between steel tube and concrete core is the discussing issue for understanding the behaviour of concrete-filled steel tube columns (CFST). Both material and geometric nonlinearities are considered in the analyses. The numerical results indicate good agreement with the experimental data. The plastic damage model can be used to predict the nonlinear response of concrete in CFST columns subjected to axial compressive loading. Length of the column varied from 2m to 4m. Boundary conditions were enforce with displacement $\delta x = \delta y = \delta z = 0$ on the bottom surface. The top surface of the column is fixed with $\delta x = \delta y = 0$ allowing displacement to take place in z directions. It has been found that thickness and diameter has great influence on strength of CFST column. The results obtained from FEA values are found very close with experiment values. This gap is because of imperfection in the input data. [20]

Patidar, (2012) studied the behaviour of concrete filled rectangular steel tube column. The FEA modelling using ANSYS software was adopted to investigate the load versus lateral deflection behaviour of the composite sections. The effects of steel tube thickness and strength of in-filled concrete tubes are examined. There were six columns. The size of the column is 140mm x 160mm x 1500mm and the grades of concrete infill are M20, M30 and M40. The thickness of the tube is taken as 2mm, 3mm, 4mm, 5mm and 6mm and the D/t ratio i.e. slenderness ratio varies from 26.67 to 80. Non-linear buckling analysis was performed to investigate the load versus deflection graph of the column. The ball and bolted end conditions are considered as pinned end conditions. The pin ended boundary condition has been modelled by restraining all the translational degrees of freedom and rotational degree of freedom of the nodes at both ends, except the translational degree of freedom in the axial direction at the top end of the column. Since the load is applied from the top of the column the translational degree of freedom has been released. The nodes other than the two ends are free to translate and rotate in x, y and z directions The finite element proposed model showed the resistance to deformation when concrete is used as infill material and deformation decreases when an increase in the grade of concrete. The hollow steel tube column however deformed to a greater extent as compared with the column having the in fill material. The 6mm thick column showed good response against deformation because of D/t ratio. [19]

Bukovska, (2012) studied the influence of the concrete strength on the behaviour of steel tubular columns filled with concrete. This paper deals with the effectiveness of using circular steel columns filled by high strength concrete in case of structural members subjected to compression. The paper was worked out within the research programme focused on true behaviour of steel tubular columns filled by concrete. Attention is focused on influence investigation of concrete strength on the behaviour of columns. For the loading tests the tubes of the diameter of 159mm and the thickness of 4.5mm with the buckling length of 3000mm were used. Total of 18 test specimens were tested within the analysis. One half of the test specimens were tubes of steel grade S235, other specimens were tubes of steel grade S355. The specimens were divided into three groups of six pieces. In combination with the two classes of steel strength six partial experiments were achieved. The paper included the interpretation and evaluation of the results of experimental analysis, initial results of numerical model and sensitivity analysis. Circular steel tubes filled by normal concrete and circular steel tubes filled by high-strength

concrete have been taken into account within the solution. The behaviour of tubular columns filled by concrete was compared based on the results of experimental analysis. The behaviour of columns without concrete was included into comparison. Numerical model has been developed in order to ensure consistency of the output of the numerical calculation and the data obtained at the test specimens. Numerical model has been developed in program ATENA 3D, which is determined for nonlinear finite element analysis of structures. Finally sensitivity analysis is presented which gives some information about influence of input parameters on the buckling strength. At the conclusion parameters with the greatest influence on the buckling resistance are discussed whereas the efficiency of using high-strength concrete is observed. [4]

El-Heweity, (2012) presented a numerical study to investigate the performance of circular high strength steel tubes filled with concrete (CFST) under monotonic axial loading. A model is developed to implement the material constitutive relationships and non-linearity. A powerful finite element technique using 'ANSYS Software' is utilized. Calibration against previous experimental data showed good agreement. A parametric study was then conducted using the model and compared with codes provisions. Strength and ductility of confined concrete are of primary concern. Variables considered are yield stress of steel tube and column diameter. The assessment of column performance is based on axial load carrying capacities and enhancements of both strength and ductility due to confinement. Two parameters namely strength enhancement factor (K_f) and ductility index (μ) are clearly defined and introduced for assessment. Results indicate that both concrete strength and ductility of CFST columns are enhanced but to different extents. The ductile behaviours are significantly evident. The increase in yield stress of steel tube has a minimal effect on concrete strength but pronounced effect on concrete ductility. However, reduction in ductility is associated with using high-tensile steel of Grade 70. The overall findings indicated that the use of high-strength tube in CFST columns is not promising. This finding may seriously be considered in seismic design. [9]

Alani and Agarwal, (2013) presented non-linear finite element study on circular concrete filled steel tubular columns. In this research modelling of 11 circular cross-section model of the columns, these models are taken from pre-publication research, the models been simulated nonlinearly by the finite element method, with the help of the ANSYS software. Models has been loaded in a concentric axial compression way, the

failure loads were extracted, and has been compared to the results obtained from the experimental data. It been found from the nonlinear modelling by ANSYS program a significant influence of the proportion of the D/t ratio on the axial load capacity of the concrete filled steel tubular, where concluded that the axial load capacity of the columns increases significantly when lowering the value of the of D/t under the value 47, but when increasing the value of the D/t over 47 the axial load capacity of the columns increases in small rates. All the specimens been simulated had the length to diameter ratio (L/D) not exceeding the value of 4.5 to act as a short column, and, therefore, no slenderness effect would be taken in account. It was found that results of the experimental test and the simulation showed good agreement. Concrete filled steel tubular columns axial capacity significantly affected with the cross-section of the column, concrete compressive strength and yield strength of the steel tubes. [1]

Singh and Gupta, (2013) presented the numerical investigation into the behaviour of rectangular concrete filled steel tubular (CFST) short columns loaded in axial compression. Nonlinear finite-element analysis is performed for the compression process using commercial software ABAQUS 6.9. A total of 16 specimens of different steel tube sizes, wall thickness, and length and filled with normal as well as high strength concrete are chosen for modelling from the available literature. The proposed model is validated by comparing its results with those of the corresponding experimental specimens. It was observed that the computational model was able to map the deformed shapes and the load deformation pattern of the concrete filled steel tubular columns across different column sizes and filled with different grades of concrete. The average value of ratio of peak load of ABAQUS to the peak load of experimental was obtained as 0.954, which indicates a good correlation between the experimental and numerically simulated results. Hence, a good agreement was also observed between the experimental and predicted peak axial load capacities. [22]

Tao et al., (2013) studied finite element modelling of concrete filled steel stub columns under axial compression. A wide range of experimental data is collected in this paper and used to develop refined FE models to simulate CFST stub columns under axial compression. The simulation is based on the concrete damaged plasticity material model, where a new strain hardening/softening function is developed for confined concrete and new models are introduced for a few material parameters used in the concrete model.

ABAQUS software was used to made FE model of concrete filled steel tubular columns. The prediction accuracy from the current model is compared with that of an existing FE model, which has been well established and widely used by many researchers. Further research was required to measure the lateral expansion of concrete inside a steel tube during the loading process. A model may be put forward accordingly to describe the axial strain–lateral strain relationship of the core concrete in CFST columns. The comparison indicates that the new model was more versatile and accurate to be used in modelling CFST stub columns, even when high-strength concrete and/or thin-walled tubes were used. [24]

Evirgen et al., (2014) investigated structural behaviour of concrete filled steel tube sections under axial compression. In this study, compressive strength, modulus of elasticity and steel tension coupon tests were performed to determine material properties. Sixteen hollow cold formed steel tubes and 48 concrete filled steel tube specimens are used for axial compression tests. The effect off width/thickness (b/t) ratio, the compressive strength of concrete and geometrical shape of cross-section parameters on the ultimate loads, axial stress, ductility and buckling behaviour were investigated. Circular, hexagonal, rectangular and square sections, 18.75, 30.00, 50.00, 100.00 b/t ratio values and 13, 26, 35 MPa concrete compressive strength values were chosen for the experimental procedure. Analytical model of specimens were also developed using the finite element software ABAQUS and then results were compared. It was found that approximately 15-20% or less differences were generally obtained between experimental and FEM results. However, some specimens approached to almost 40%. Core concrete can behave as non-brittle material due to elimination of the desiccation of concrete moisture by steel tube in certain cases. Circular specimens were the most effective samples according to both axial stress and ductility values. The concrete in the tubes has experienced considerable amount of deformations which was not expected from such a brittle material in certain cases. The results provide an innovative perspective on using cold form steel and concrete together as a composite material. [10]

Dai et al., (2014) presented a non-linear finite element model used to predict the behaviour of slender concrete filled steel tubular columns with elliptical hollow sections subjected to axial compression. The accuracy of the FEM was validated by comparing the numerical prediction against experimental observation of eighteen elliptical CFST

columns which carefully represent typical section sizes and member slenderness. In total, eighteen slender elliptical CFST columns, with two hollow section sizes (150mm x 75mm x 4mm, 200mm x 100mm x 5mm), three column lengths (1.5m, 1.8m and 2.5m) and three nominal concrete strength (30, 60 and100 MPa) were tested to investigate the axial compressive behaviour and failure modes. The adaptability to apply the current design rules provided in Eurocode 4 for circular and rectangular CFST columns to elliptical CFST columns were discussed. Finite element model was developed by ABAQUS software in order to validate the results with experimental results. A parametric study was carried out with various section sizes, lengths and concrete strength in order to cover a wider range of member cross-sections and slenderness which is currently used in practices to examine the important structural behaviour and design parameters, such as column imperfection, non-dimension slenderness and buckling reduction factor, etc. Both experimental and numerical modelling results demonstrated that the failure mode of a slender CFST column under compressive loads was global buckling with the first buckling mode shape. It was conclude that the simplified design method provided in Eurocode 4 may be used for axial compressive behaviour design of elliptical CFST columns and the initial imperfection has a significant effect to the axial compressive behaviour of slender elliptical CFST columns. Initial imperfection of Le/2000 should be used for the FE modelling. Where Le was effective length of the concrete filled steel tubular column. It was also concluded that the design rules given in Eurocode 4 for circular and rectangular CFST columns may be adopted to calculate the axial buckling load of elliptical CFST columns although using the imperfection of length/300 specified in the Eurocode 4 might be over- conservative for elliptical CFST columns with lower non-dimensional slenderness. [7]

2.3 GAPS IN RESEARCH WORK

Many experimental and analytical works has been done by many researchers in the area of concrete filled steel tubular columns under axial loading. The concrete filled steel tubular column has in the recent years evolved as alternative to the conventional methods in vogue. It is structural member which resists the load from super structures. Steel sections with concrete infill are being increasingly used as structural members, since filling the steel section with concrete increases both its strength and ductility without increasing the section size. Many researchers found that the CFST column system has many advantages compared with the ordinary steel or the reinforced concrete system due

to its high-strength, stiffness, ductility, and better seismic resistance. Since steel confines the concrete, the use of formwork can be discarded. Some researchers have also investigated or work on the area of the failure mode of the concrete filled steel tubular columns and some are work to improve the performance of concrete filled steel tubular columns by applying different materials.

This research is concerned with the finite element modelling of concrete filled steel tubular columns under axial loading. The use of concrete filled steel tubes have been studied extensively in previous studies. However, many researchers performed experimentally and analytically the concrete filled steel tubular beams/columns but limited work is done on the study of axially loaded concrete filled steel tubular columns by using FE modelling.

2.4 CLOSURE

The literature review has suggested that use of a finite element modelling of concrete filled steel tubular columns is indeed feasible. So it has been decided to use ATENA for the FE modelling. With the help of this software study of concrete filled steel tubular columns has been done. ATENA also helps in FE modelling and meshing inside the surface of element. It gives the load deflection curve and gives the values of stresses and strains at every step. Concrete filled steel tubular columns modelled discretely will be developed with results compared to the experimental work done by Uy et al. (2009). The load-deformation curve of the experimental work will be compared to analytical predictions to calibrate the FE model for further use.

CHAPTER3 FE MODELLING OF CFST COLUMN

3.1 GENERAL

Modelling concrete filled steel tubular column presented in this chapter refers to the column detail, material properties and loading conditions as taken in the experimental study conducted by **Uy et al. (2009)**. The control concrete filled steel tubular column under axial loading was taken and analyzed by finite element method (FEM) using the commercial available software **ATENA**.

This chapter also discusses the theory related to ATENA and information about finite elements currently implemented in ATENA. All the necessary steps to create these models are explained in detail and the steps taken to generate the analytical load-deformation response of the model are discussed.

3.2 GENERAL DESCRIPTION OF THE STRUCTURE

In the experimental program conducted by Uy et al. (2009), behaviour of concrete filled steel tubular columns under axial loading was studied. Six specimens were fabricated i.e. S1-1a, S1-1b, S1-2a, S1-2b, S1-3a and S1-3b. Hence these specimens were divided into three series. In first series, S1-1a and S1-1b have same size but their characteristic compressive strength was different. Similarly in second series, S1-2a and S-2b have also same size but there compressive strength was different. Lastly, in third series, S1-3a and S1-3b have also same size but there compressive strength was different. In these concrete filled steel tubular columns, steel tube made of stainless steel having yield stress of 390.3 MPa. Details of the specimen are given in Table 3.1.

3.2.1 MATERIAL PROPERTIES

Materials used for the fabrication of concrete filled steel tubular columns are steel tube of required size and concrete mix of suitable grade. Cylindrical compressive strength are 36.3 MPa and 75.4 MPa. The basic material properties are as follows.

Modulus of elasticity of steel, E_s = 210000 MPa
Modulus of elasticity of concrete (E_c) for 36.3 MPa compressive strength = 33900 MPa
Modulus of elasticity of concrete (E_c) for 75.4 MPa compressive strength = 37900 MPa

Yield strength of the steel (σ_y) = 390.3 MPa

3.2.2 MODEL GEOMETRY

There are six specimens. Size of different columns according to their compressive strength are given in Table 3.1 given below.

Table 3.1. Details of specimen and test results. [25]

No.	Specimen Label	λ (Slenderness ratio)	Size of Column (B x t)	Length (L) (mm)	Compressive strength of CFST (MPa)
1	S1-1a	15.2	100.3 x 2.76	440	36.3
2	S1-1b	15.2	100.3 x 2.76	440	75.4
3	S1-2a	46.3	100.3 x 2.76	1340	36.3
4	S1-2b	46.3	100.3 x 2.76	1340	75.4
5	S1-3a	87.7	100.3 x 2.76	2540	36.3
6	S1-3b	87.7	100.3 x 2.76	2540	75.4

Hence all these columns are square. Fig.3.1 shows square column section. B is the width of the CFST column. Since column is square, hence all sides have same width. t is the thickness of the steel tube. L is the length of the CFST column.

λ is the slenderness ratio. As slenderness ratio is defined as the ratio of effective length to the least lateral dimension. Slenderness ratio given by Uy et al. (2009)

$$\lambda = 2\sqrt{3}\, L/B$$

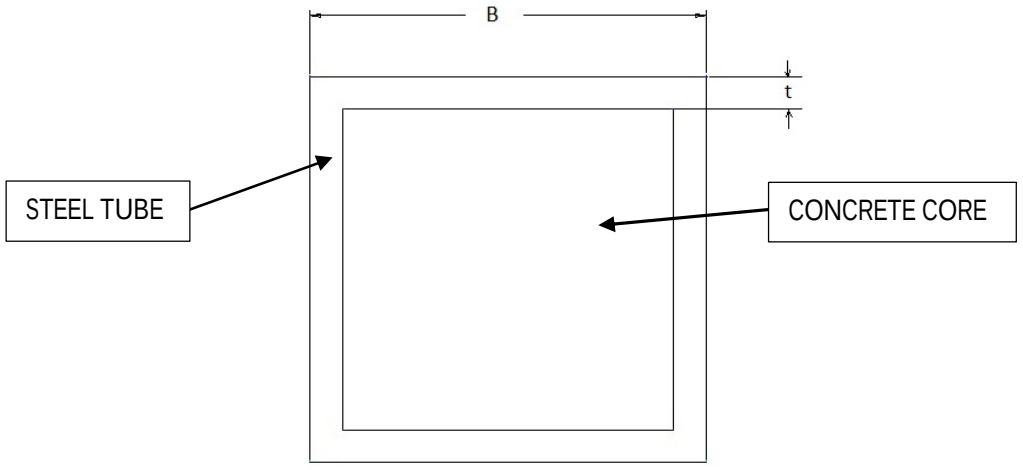

Fig.3.1 Top view of CFST column

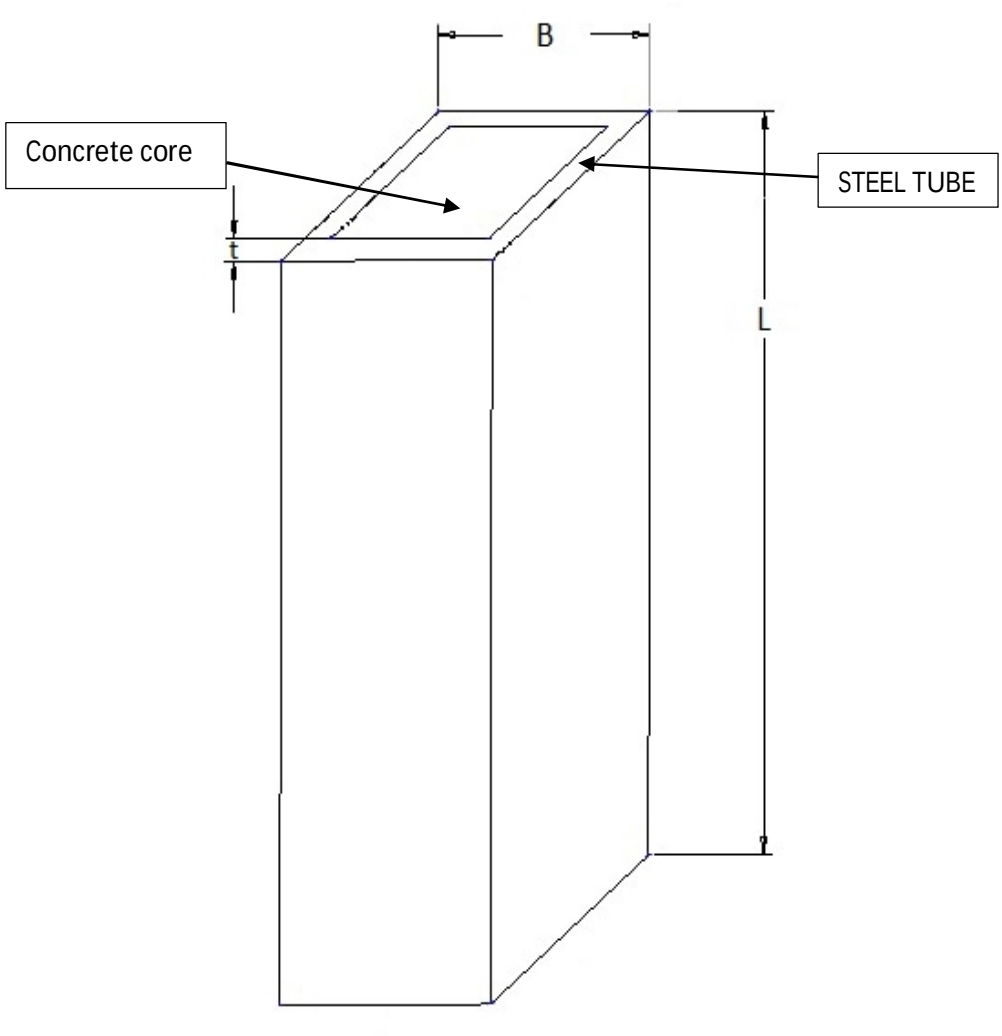

Fig.3.2 Isometric view of CFST column

Fig.3.2 shows isometric view of CFST column. In this isometric view, there is a concrete core and this concrete core is confined by steel tube. Fig.3.3 shows full geometry of CSFT column. As two faces are there (concrete and steel faces), it is difficult to provide constant loading to both faces at once. Hence, steel plates must be placed at the top and bottom of CFST column so as to provide constant loading. Where T, the thickness of the steel plate is 10mm in every specimen. Boundary conditions are enforce with displacement $\delta x = \delta y = \delta z = 0$ on the bottom surface. The top surface of the column is fixed with $\delta x = \delta y = 0$ allowing displacement to take place in z direction because the length of the column is in z- direction.

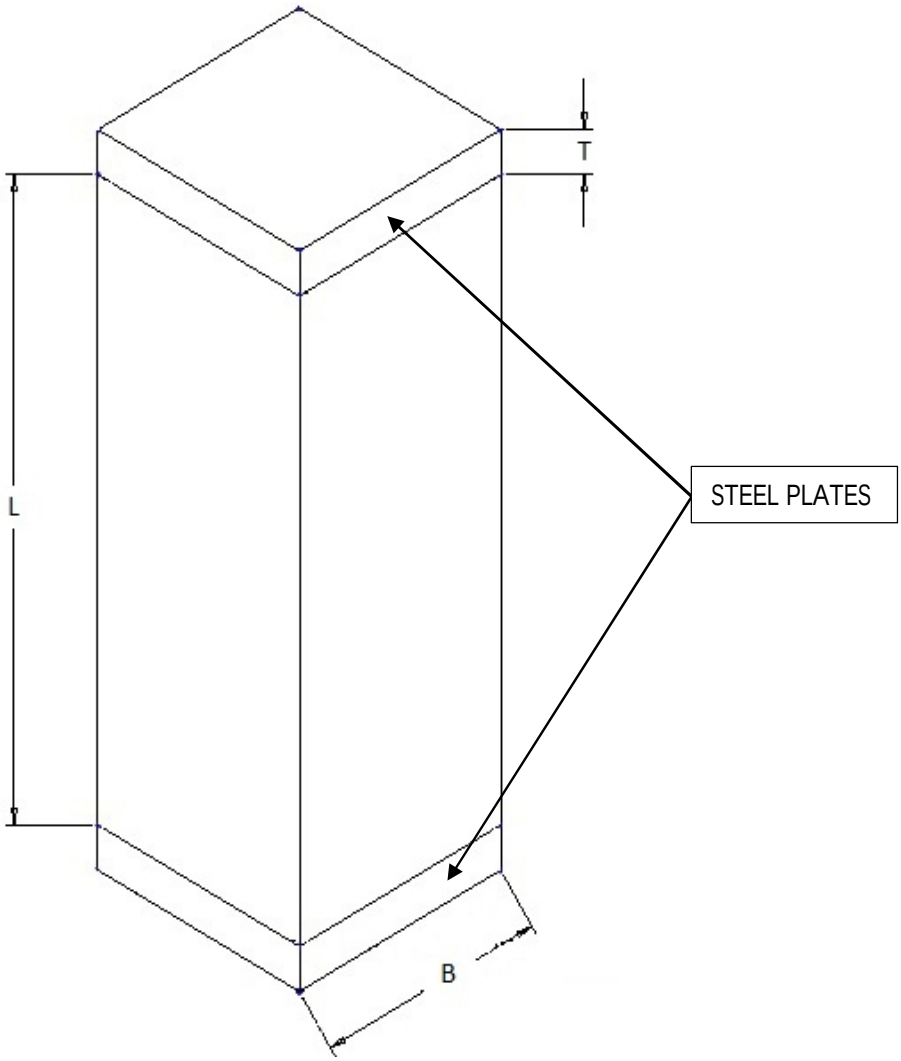

Fig.3.3. Full geometry of CFST column

3.3 INTRODUCTION TO FE MODELLING

Engineering analysis of mechanical systems have been addressed by deriving differential equations relating the variables of through basic physical principles such as equilibrium, conservation of energy, conservation of mass, the laws of thermodynamics, Maxwell's equations and Newton's laws of motion. However, once formulated, solving the resulting mathematical models is often impossible, especially when the resulting models are nonlinear partial differential equations. Only very simple problems of regular geometry such as a rectangular of a circle with the simplest boundary conditions were tractable. But FEM made this easy to solve the problems by giving approximate solution by discretization of the structure.

3.3.1 FINITE ELEMENT METHOD

FEM is a numerical technique to find approximate solutions for boundary value problems, for partial differential equations and also for integral equations. These differential equations are solved by either eliminating the differential equations completely or by rendering these differential equations into ordinary differential equations which are then numerically integrated using standard techniques.

FE Method works in the following way:

1. Discretize the Continuum.
2. Select Interpolation Functions.
3. Find the material properties.
4. Assemble the Material Properties to obtain the System Equations.
5. Impose the Boundary Conditions.
6. Solve the System Equations.
7. Make Additional Computations if desired.

3.3.2 APPLICATIONS OF FINITE ELEMENT METHOD

1. FEM allows detailed visualization of where structures bend or twist, and indicates the distribution of stresses and displacements.
2. FEM can readily handle very complex geometry.
3. FEM can also handle complex loading.
4. FEM allows entire designs to be constructed, refined, and optimized before the design is manufactured.
5. FEM provides stiffness and strength visualizations.
6. FEM also provides a wide range of simulation options for controlling the complexity of both modelling and analysis of a system.

3.4 FINITE ELEMENT MODELLING

The finite element method (FEM) is the dominant discretization technique in structural mechanics. The concept of FEM modelling is the division of mathematical model into non-overlapping components of simple geometry. The response of each element is expressed in terms of a finite number of degrees of freedom characterized as the value of an unknown function.

The finite element method is well suited for superimposition of material models for the constituent parts of a composite material. Advanced constitutive models implemented in the finite element system ATENA serve as rational tools to explain the behaviour of connection between steel and concrete. Nonlinear simulation using the models in ATENA can be efficiently used to support and extend experimental investigations and to predict behaviour of structures and structural details.

Several constitutive models covering these effects are implemented in the computer code ATENA, which is a finite element package designed for computer simulation of concrete structures. The graphical user interface in ATENA provides an efficient and powerful environment for solving many anchoring problems. ATENA enables virtual testing of structures using computers, which is the present trend in the research and development world. Utilization of ATENA for simulation of connections between steel and concrete is good. In ATENA, concrete is represented by solid brick element, reinforcement by bar elements and FRP by shell elements. Material properties play an important role in modelling of a structure.

3.5 Material Models

The program ATENA offers a variety of material models for different materials and purposes. The most important material models in ATENA for concrete filled steel tubular columns are concrete and steel tube. These advanced models considers all the important aspects of real material behaviour in tension and compression.

3.5.1 MODELLING OF CONCRETE [3]

1) Geometry of the Concrete

Element geometric modelling of concrete has been done using 3D solid brick element with 8 up to 20 nodes in ATENA, as shown in Fig.3.4.

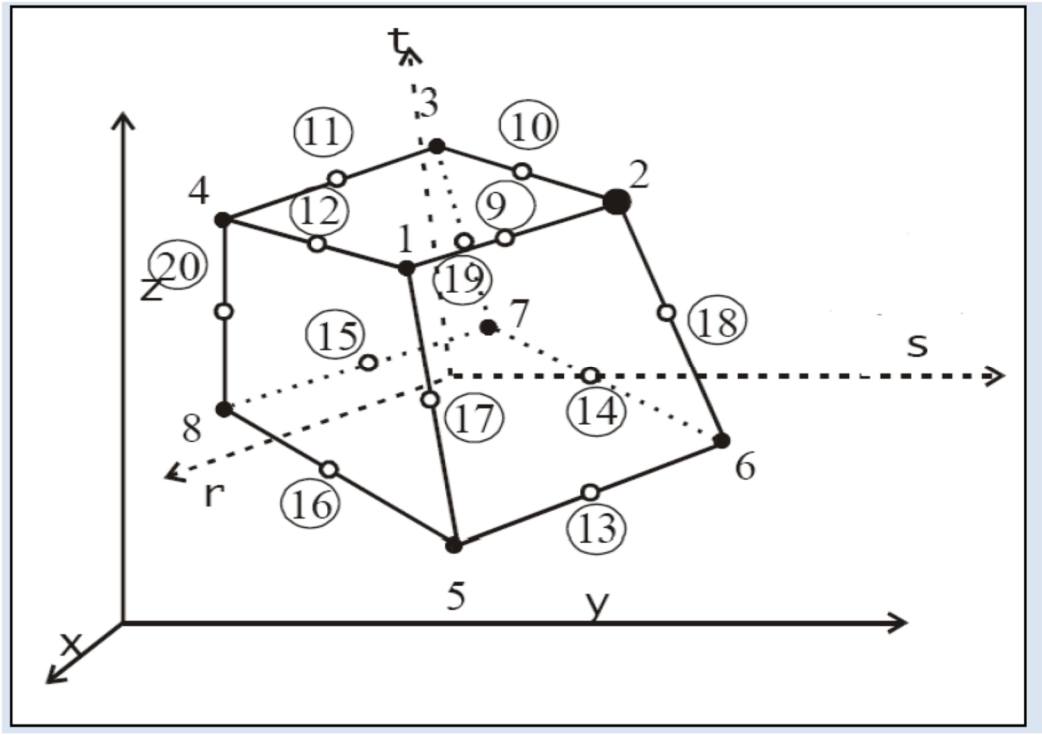

Fig.3.4 Geometry of brick elements. [3]

2) Element Properties

3D solid brick element having three degree of freedom at each node: translations in the nodal x, y and z directions. This is an isoperimetric elements integrated by Gauss integration at integration points. This element is capable of plastic deformation, cracking in three orthogonal directions, and crushing. The most important aspect of this element is the treatment of non-linear material properties.

3) Element Interpolation function

3D solid brick element interpolation functions for all variants of the elements are given below:

N1= (1/8) (1+r) (1+s) (1+t) N2= (1/8) (1-r) (1+s) (1+t)

N3= (1/8) (1-r) (1-s) (1+t) N4= (1/8) (1+r) (1-s) (1+t)

N5= (1/8) (1+r) (1+s) (1-t) N6= (1/8) (1-r) (1+s) (1-t)

N7= (1/8) (1-r) (1-s) (1-t) N8= (1/8) (1+r) (1-s) (1-t)

3.5.2 MODELLING OF STEEL TUBE

Modelling of steel tube is given by 3D Bilinear Steel Von Mises in ATENA software. In ATENA, this material modelling is used to model the hollow steel tube before the

concrete is encased into it. Stress strain and biaxial failure law for 3D bilinear steel Von Mises material model are shown in Fig. 3.5.

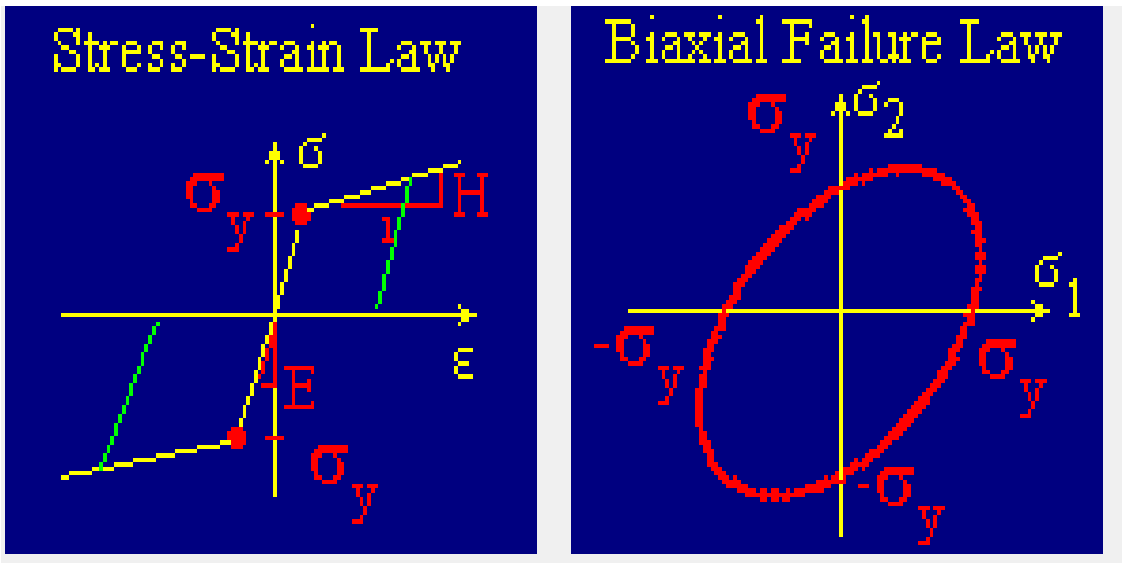

Fig.3.5 Stress strain and biaxial failure law for 3D bilinear steel Von Mises

3.5.2 MODELLING OF STEEL PLATE

Modelling of steel tube is given by 3D elastic isotropic material model in ATENA software. Elastic modulus of steel is 21 GPa and Poisson's ratio is 0.2. Stress strain law for 3D isotropic material is shown in Fig.3.6.

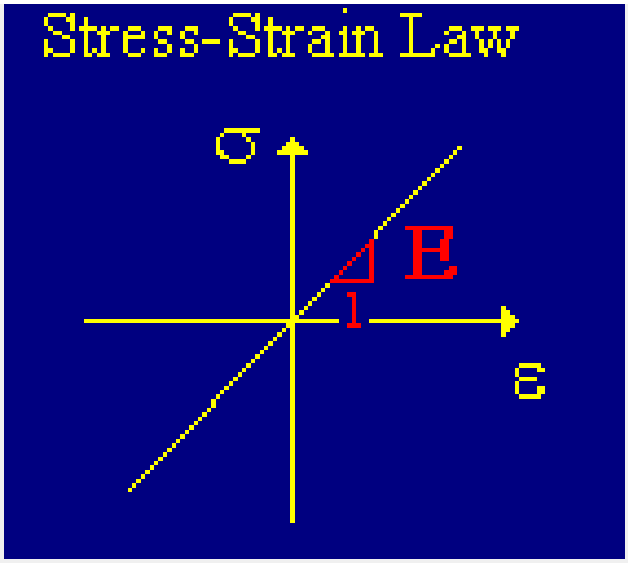

Fig.3.6 Stress strain law for 3D isotropic material model

3.6 STRESS - STRAIN RELATIONS FOR CONCRETE [3]

Concrete exhibits a large number of micro-cracks, especially, at the interface between coarser aggregates and mortar, even before subjected to any load. The presence of these micro-cracks has a great effect on the mechanical behaviour of concrete, since their propagation during loading contributes to the nonlinear behaviour at low stress levels and causes volume expansion near failure. Many of these micro-cracks are caused by segregation, shrinkage or thermal expansion of the mortar. Some micro-cracks may develop during loading because of the difference in stiffness between aggregates and mortar. Since the aggregate-mortar interface has a significantly lower tensile strength than mortar, it constitutes the weakest link in the composite system. This is the primary reason for the low tensile strength of concrete.

The response of a structure under load depends to a large extent on the stress-strain relation of the constituent materials and the magnitude of stress. Since concrete is used mostly in compression, the stress-strain relation in compression is of primary interest.

3.6.1 EQUIVALENT UNIAXIAL LAW [3]

The nonlinear behaviour of concrete in the biaxial stress state is described by means of the so called effective stress σ_c^{ef}, and the equivalent uni-axial strain ε^{eq}. The effective stress is in most cases a principal stress. The equivalent uni-axial strain is introduced in order to eliminate the Poisson's effect in the plane stress state.

$$\boldsymbol{\varepsilon^{eq} = \sigma ci / E_{ci}}$$

The equivalent uni-axial strain can be considered as the strain, that would be produced by the stress σ_{ci} in a uni-axial test with modulus associated E_{ci} with the direction i. Within this assumption, the nonlinearity representing damage is caused only by the governing stress σ_{ci}. The complete equivalent uni-axial stress-strain diagram for concrete is shown in Fig.3.7. The numbers of the diagram parts in Fig.3.7 (material state numbers) are used in the results of the analysis to indicate the state of damage of concrete.

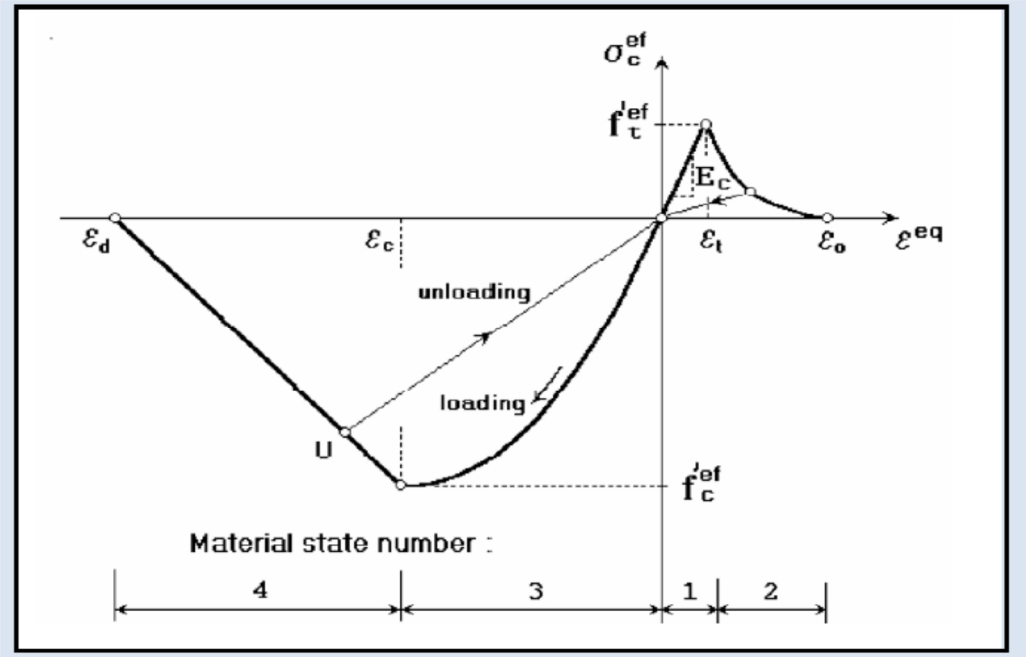

Fig. 3.7 Equivalent uni-axial stress-strain law [3]

Unloading is a linear function to the origin. An example of the unloading point U is shown in Fig.3.7. Thus, the relation between stress σ and strain ε^{eq} is not unique and depends on a load history. A change from loading to unloading occurs, when the increment of the effective strain changes the sign. If subsequent reloading occurs the linear unloading path is followed until the last loading point U is reached again. Then, the loading function is resumed. The peak values of stress in compression f_c^{ef} and in tension f_t^{ef} are calculated according to the biaxial stress state. Thus, the equivalent uni-axial stress-strain law reflects the biaxial stress state.

3.6.2 BIAXIAL STRESS FAILURE CRITERION OF CONCRETE [3]

1) Compressive Failure

A biaxial stress failure criterion according to KUPFER et al. (1969) is used as shown in Figure3.8.

In the compression-compression stress state the failure function is

$$\mathbf{f'_c{}^{ef} = [(1+3.65a) / (1+a)\ 2]\ f'_c\ ;} \qquad \mathbf{a = (\sigma_{c1}/\sigma_{c2})} \tag{3.1}$$

Where σ_{c1}, σ_{c2} are the principal stresses in concrete and f_c is the uni-axial cylinder strength. In the biaxial stress state, the strength of concrete is predicted under the assumption of a proportional stress path.

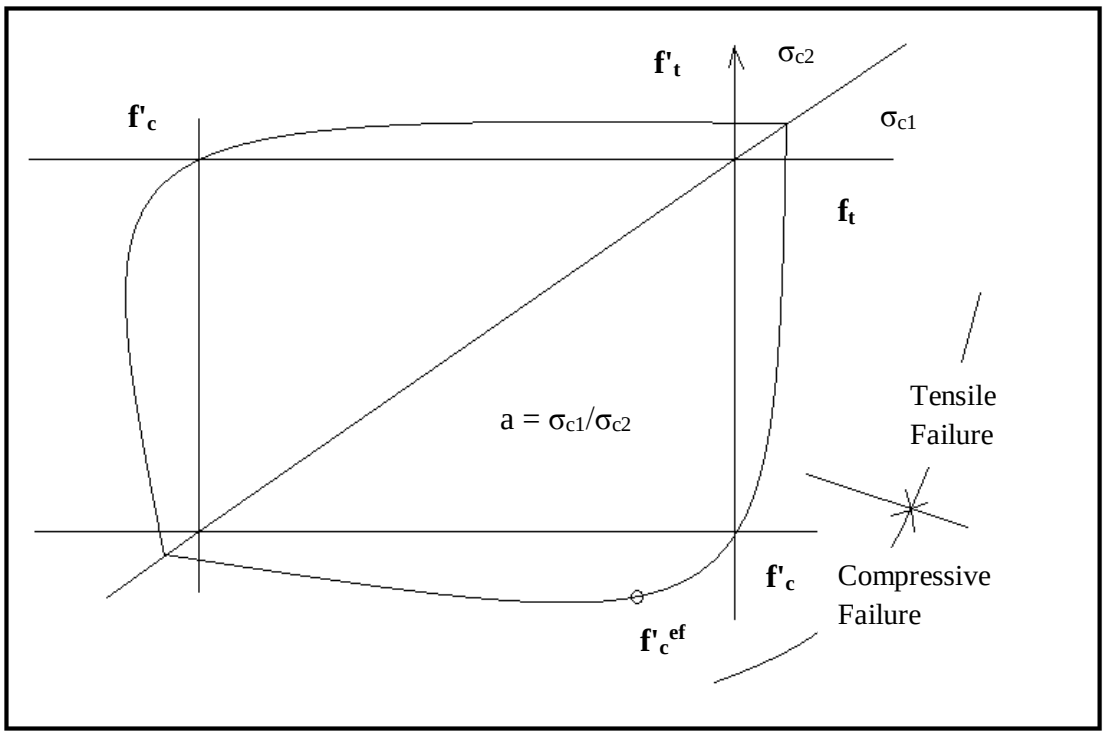

Fig.3.8 Biaxial failure functions for concrete [3]

In the tension-compression state, the failure function continues linearly from the point $\sigma_{c1} = 0$, $\sigma_{c2} = f'_c$, into the tension-compression region with the linearly decreasing strength:

$$\mathbf{f'_c{}^{ef} = f'_c r_{ec}, \qquad r_{ec} = [1 + 5.3278(\sigma c_1 / f'_c)]} \tag{3.2}$$

Where rec is the reduction factor of the compressive strength in the principal direction 2 due to the tensile stress in the principal direction 1.

2) Tensile failures

In the tension-tension state, the tensile strength is constant and equal to the uniaxial tensile strength f'_t. In the tension-compression state, the tensile strength is reduced by the relation:

$$\mathbf{f'_t{}^{ef} = f'_t r^{et}} \tag{3.3}$$

Where ret is the reduction factor of the tensile strength in the direction 1 due to the compressive stress in the direction 2. The reduction function has one of the following forms.

$$\mathbf{r^{et} = 1 - 0.8\,(\sigma_{c2} / f'_c)} \tag{3.4}$$

$$\mathbf{r^{et} = [A + (A - 1)\,B] / AB;\ B = Kx + A\ ;\ x = \sigma_{c2} / f'_c} \tag{3.5}$$

The relation in eq. (3.4) represents the linear decrease of the tensile strength and eq. (3.5) represents the hyperbolic decrease.

Two predefined shapes of the hyperbola are given by the position of an intermediate point r, x.

Constants K and A define the shape of the hyperbola. The values of the constants for the two positions of the intermediate point are given in the Table 3.2.

Table 3.2. Parameters and points of hyperbola in tensile failure of concrete.

TYPE	POINT		PARAMETERS	
	r	X	A	K
A	0.5	0.4	0.75	1.125
B	0.5	0.2	1.0625	6.0208

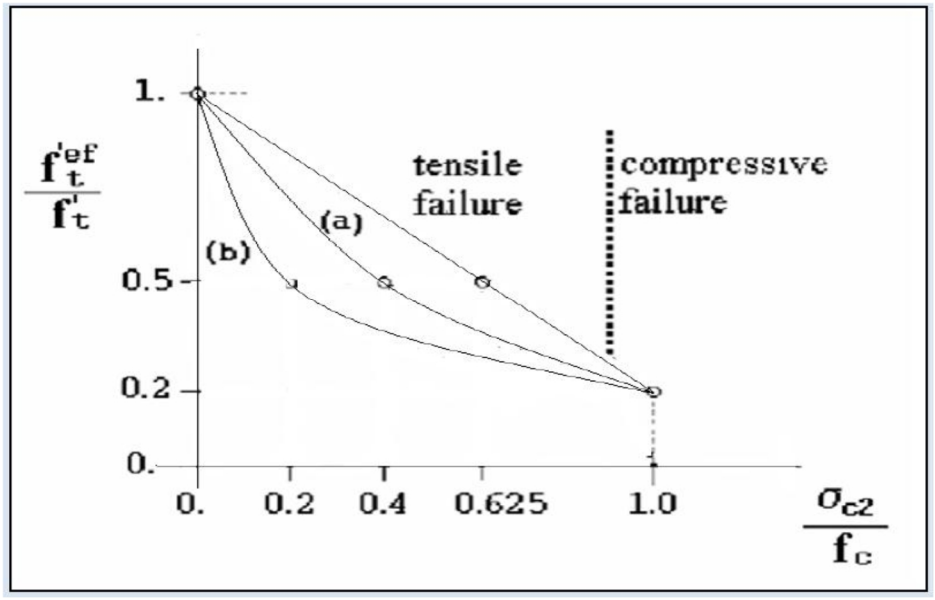

Fig.3.9 Tension Compression failure function of concrete [3]

3.6.3 TENSION BEFORE CRACKING

The behaviour of concrete in tension without cracks is assumed linear elastic. E_c is the initial elastic modulus of concrete, f'^{ef}_t is the effective tensile strength derived from the biaxial failure function already describe above.

$$\sigma_c^{ef} = E_c\ \varepsilon_{eq},\ 0 < \sigma_c < f'^{ef}_t$$

3.6.4 TENSION AFTER CRACKING

A fictitious crack model is based on a crack-opening law and fracture energy. This formulation is suitable for modelling of crack propagation in concrete. It is used in combination with the crack band. It is a region (band) of material, which represents a discrete failure plane in the finite element analysis. In tension it is a crack, in compression it is a plane of crushing. In reality these failure regions have some dimension. However, since according to the experiments, the dimensions of the failure regions are independent on the structural size, they are assumed as fictitious planes. In case of tensile cracks, this approach is known as rack "crack band theory**", (BAZANT OH 1983).**

Here is the same concept used also for the compression failure. The purpose of the failure band is to eliminate two deficiencies, which occur in connection with the application of the finite element model: element size effect and element orientation effect.

1) Element size effect.

The direction of the failure planes is assumed to be normal to the principal stresses in tension and compression, respectively. The failure bands (for tension L_t and for compression L_c) are defined as projections of the finite element dimensions on the failure planes.

2) Element Orientation Effect.

The element orientation effect is reduced, by further increasing of the failure band for skew meshes, by the following formula (proposed by (**CERVENKA et al. 1995).**

$$\mathbf{L_t = \gamma L_t,\ L_c = \gamma L_c}$$

$$\gamma = 1 + (\gamma_{max} - 1)\ (\theta / 45),\ \theta\ \varepsilon\ (0; 45) \qquad (3.6)$$

An angle θ is the minimal angle (min ($\theta 1$, $\theta 2$)) between the direction of the normal to the failure plane and element sides. In case of a general quadrilateral element the element sides directions are calculated as average side directions for the two opposite edges. The above formula is a linear interpolation between the factor γ=1.0 for the

direction parallel with element sides, and $\gamma = \gamma_{max}$, for the direction inclined at 45^0. The recommended (and default) value of γ_{max} =1.5.

3.7 MATERIAL PROPERTIES

Concrete, steel tube and steel plates at top and bottom of the column have been used to model the concrete filled steel tubular columns. The specification and the properties of these materials are as under:

1) Concrete

In ATENA, concrete material is modelled as a 3D nonlinear cementitious2. The physical properties of 3D nonlinear cementitious2 material are given in Table 3.3.

2) Steel tube

Steel tube having yield stress 390.3 MPa taken in ATENA Software. The properties of steel tube are shown in Table 3.4.

Table 3.3. Properties of concrete.

PROPERTIES	VALUE
Elastic Modulus (For 36.3 MPa compressive strength)	33900 MPa
Elastic Modulus (For 75.4 MPa compressive strength)	37900 MPa
Poisson Ratio	0.2
Tensile Strength	6.083 MPa
Specific Fracture Energy	3.841×10^{-5} MN/m
Critical Compressive Displacement	5×10^{-4}
Reduction of Compressive Strength	0.8
Plastic Strain at Compressive Strength	6.681×10^{-4}
Specific Material Weight	23 KN/m^3
Coefficient of Thermal Expansion	1.200×10^{-5} 1/K
Fixed Crack Model Coefficient	1

Table 3.4 Material Properties of steel

PROPERTIES	VALUE
Elastic modulus	210000 MPa
Yield Strength	390.3 MPa
Specific Material weight	0.0785 MN/m^3
Coefficient of Thermal Expansion	1.2 x 10^{-5} 1/K

3) Steel Plate

The function of the steel plate in the ATENA is for support and for loading. Here, the property of steel plate is same as the steel tube.

3.8 FE MODELLING OF CONCRETE FILLED STEEL TUBULAR COLUMNS IN ATENA

The ATENA program, which is determined for nonlinear finite element analysis of structures, offers tools specially designed for computer simulation of concrete, reinforced concrete and composite material structural behaviour. ATENA program system consists of a solution core and several user interfaces. The solution core offers capabilities for variety of structural analysis tasks, such as: stress and failure analysis, transport of heat and humidity, time dependent problems (creep, dynamics), and their interactions. Solution core offers a wide range of 2D and 3D continuum models, libraries of finite elements, material models and solution methods. User interfaces are specialized on certain functions and thus one user interface need not necessarily provide access to all features of ATENA solution core. This limitation is made on order to maintain a transparent and user friendly user environment in all specific applications of ATENA.

ATENA 3D program is designed for 3D nonlinear analysis of solids with special tools for composite structures. However, structures from other materials, such as soils, metals etc. can be treated as well. The program has three main functions:

A. Pre-processing

B. Run

C. Post-processing

A. **Pre-processing:** Input of geometrical objects (concrete, steel tube and steel plates), loading and boundary conditions, meshing and solution parameters.

B. **Analysis:** It makes possible a real time monitoring of results during calculations.

C**. Post-processing:** Access to a wide range of graphical and numerical results

Procedure:

In pre-processing window following steps are performed:

Step1: Geometry of FE model is created as shown in Fig.3.10.

Step2: Material properties are assigned to the various elements of the concrete filled steel tubular column.

Step3: Structural element, various supports, loadings and monitoring points are defined.

Step4: Finite element meshing parameters are given and meshing of the model is generated accordingly as shown in Fig. 3.10.

Step5: Various analysis steps are defined. The FE non-linear analysis is done in Run window. The FE non-linear static analysis calculates the effects of steady loading conditions on a structure. A static analysis can, however, include steady inertia loads (such as gravity and rotational velocity), and time-varying loads that can be approximated as static equivalent. Static analysis is used to determine the displacements, stresses, strains, and forces in structures or components by loads.

Step6: When the FE non-linear static analysis is completed the, the results are shown in third part of the ATENA i.e. Post processing. The stress- strain values at every step, crack pattern and cracks propagation at every step shown help in to analyse the behaviour of the elements at every step of load deflection. There are two monitoring points as shown in Fig.3.10. One is at the top of the column to get the axial deformation and other is at the mid height of the column to get mid height deflection.

Analysis is deformation control and value of load is checked at every step of deformation. Step size of the deformation is 0.1 mm. Firstly deformation steps are given to obtain the peak load. When peak load is obtained, mid-point monitoring point gives deflection values.

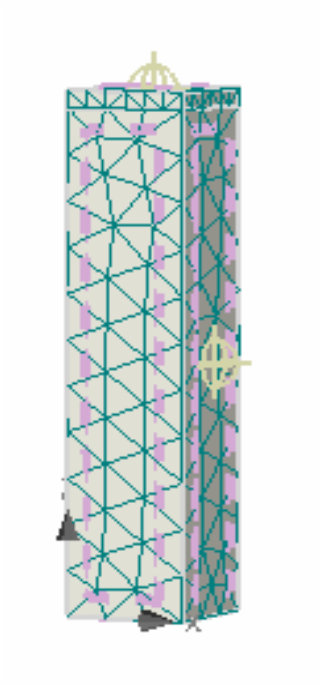

Fig.3.10 Modelling and geometry of CFST column.

3.9 METHODS FOR NON-LINEAR SOLUTION [3]

The best part of the ATENA is the simpler way of solving the non-linear structural behaviour through finite element method and its incremental loading criteria. Different methods are available in ATENA for solving non-linear equations such as, linear method, Newton-Raphson Method, Modified Newton-Raphson method, Arc Length methods are used in ATENA.

Among these the Newton-Raphson Method and Modified Newton-Raphson Method are more commonly used methods. In our present study, Newton-Raphson method is used for solving the simultaneous equations. It is an iterative process of solving the non-linear equations.

One approach to non-linear solutions is to break the load into a series of load increments. The load increments can be applied either over several load steps or over several sub steps within a load step. At the completion of each incremental solution, the

program adjusts the stiffness matrix to reflect the nonlinear changes in structural stiffness before proceeding to the next load increment.

The ATENA program overcomes this difficulty by using Full Newton-Raphson method, or Modified Newton-Raphson method, which drive the solution to equilibrium convergence (within some tolerance limit) at the end of each load increment. In Full Newton-Raphson method, it obtains the following set of non-linear equations:

$$K(p)\,\Delta p = q - f(p)$$

Where,

q is the vector of total applied joint loads,

f(p) is the vector of internal joint forces,

Δp is the deformation increment due to loading increment,

p are the deformations of structure prior to load increment,

K(p) is the stiffness matrix, relating loading increments to deformation increments.

Figure 3.11 illustrates the use of Newton-Raphson equilibrium iterations in nonlinear analysis. Before each solution, the Newton-Raphson method evaluates the out-of-balance load vector, which is the difference between the restoring, forces (the loads corresponding to the element stresses) and the applied loads. The program then performs a linear solution, using the out-of-balance loads, and checks for convergence. If convergence criteria are not satisfied, the out-of- balance load vector is re-evaluated, the stiffness matrix is updated, and a new solution is obtained. This iterative procedure continues until the problem converges. But sometimes, the most time consuming part of the Full Newton-Raphson method solution is the re-calculation of the stiffness matrix $K(p_i{-}1)$ at each iteration. In many cases this is not necessary and we can use matrix $K(p_0)$ from the first iteration of the step. This is the basic idea of the so-called Modified Newton-Raphson method. It produces very significant time saving, but on the other hand, it also exhibits worse convergence of the solution procedure. The simplification adopted in the Modified Newton -Raphson method can be mathematically expressed by:

$$K(p_i{-}1) = K(p_o)$$

The modified Newton-Raphson method is shown in Figure 3.12. Comparing Figure 3.11 and Figure 3.12, it is apparent that the Modified Newton-Raphson method converges more slowly than the original Full Newton-Raphson method. On the other

hand, a single iteration costs less computing time, because it is necessary to assemble and eliminate the stiffness matrix only once. In practice a careful balance of the two methods is usually adopted in order to produce the best performance for a particular case. Usually, it is recommended to start a solution with the original Newton-Raphson method and later, i.e. near extreme points, switch to the modified procedure to avoid divergence.

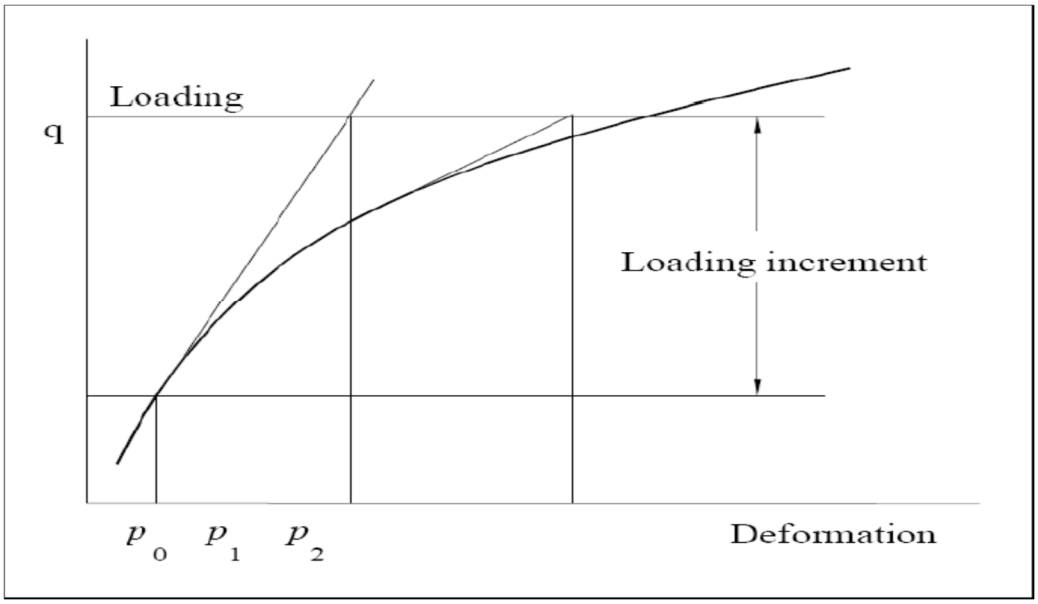

Figure 3.11 Full Newton-Raphson Method [3]

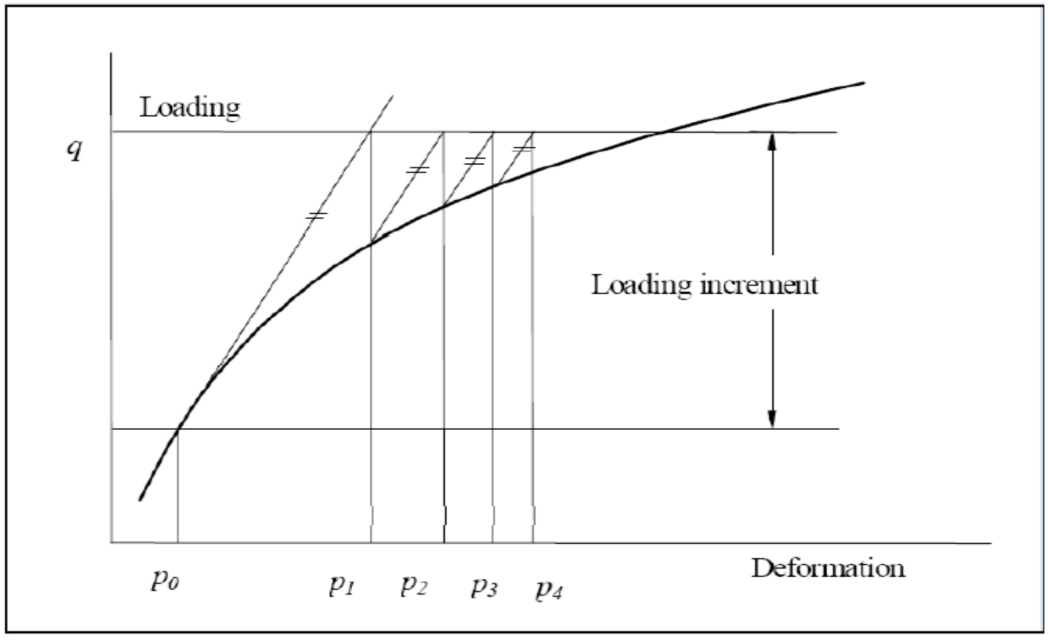

Figure 3.12 Modified Newton-Raphson Method [3]

CHAPTER 4 RESULTS AND DISCUSSIONS

4.1 GENERAL

In the present study, non-linear response of concrete filled steel tubular columns has been modelled as per details discussed in Chapter3 (3.2 General Description of Structure) under axial loading. Results of six different models has been studied and compared along with the experimental results. The objective of this study is to see the variation of load-deformation for the columns.

This chapter presents the results of Finite Element analysis of concrete filled steel tubular columns under axial load. Finite element analysis of concrete filled steel tubular columns under the static incremental loads has been performed using ATENA software. This is followed by load deformation curve obtained from the analysis. In the end the results are compared.

The load-deformation values at every step have been recorded. The load v/s deformation curves have been plotted for all models of CFST columns under axial loading and compared with each other. Subsequently these results are also compared with experimental results of "Uy et al. (2009)".

4.2 AXIAL DEFORMATION OF CFST COLUMN UNDER AXIAL LOADING

Under axial loading, six concrete filled steel tubular columns has been modelled. Finite element modelling of CFST column under axial loading has been carried out (discussed in detail in Chapter 3). Load has been applied axially on the top of the column on the steel plate.

4.2.1 AXIAL DEFORMATION OF S1-1a CFST COLUMN

Fig. 4.1 describes the way of deformations resulted by different loads. In this graph, x-axis represents deformation in mm and y-axis describes load in KN. It has been seen that deformation increases rapidly with the increase in load upto 732.5 KN which is the peak load for this CFST column, when deformation is 1.3mm. The deformation keeps on increasing even after this point but the load starts decreasing accordingly. As the analysis continued, the load carrying capacity decreased progressively. Further, the load has been found to be 634.6 KN at the deformation of 4mm.

Table 4.1. Load and deformation values of S1-1a CFST column.

S1-1a			
Load(KN)	**Deformation(mm)**	**Load(KN)**	**Deformation(mm)**
0	0	700.9	2.1
90.38	0.1	695.5	2.2
174.9	0.2	689.5	2.3
253.8	0.3	683.8	2.4
328.5	0.4	678	2.5
400	0.5	671.2	2.6
468.5	0.6	665.1	2.7
527.5	0.7	658.7	2.8
587.6	0.8	654	2.9
644.6	0.9	649.6	3
692.1	1	647.1	3.1
719.3	1.1	643.6	3.2
729.8	1.2	641.7	3.3
732.5	1.3	640.7	3.4
731.5	1.4	639.4	3.5
729	1.5	637.9	3.6
724.7	1.6	636.7	3.7
720.7	1.7	636.1	3.8
716.5	1.8	635.5	3.9
711.8	1.9	634.6	4
706.1	2		

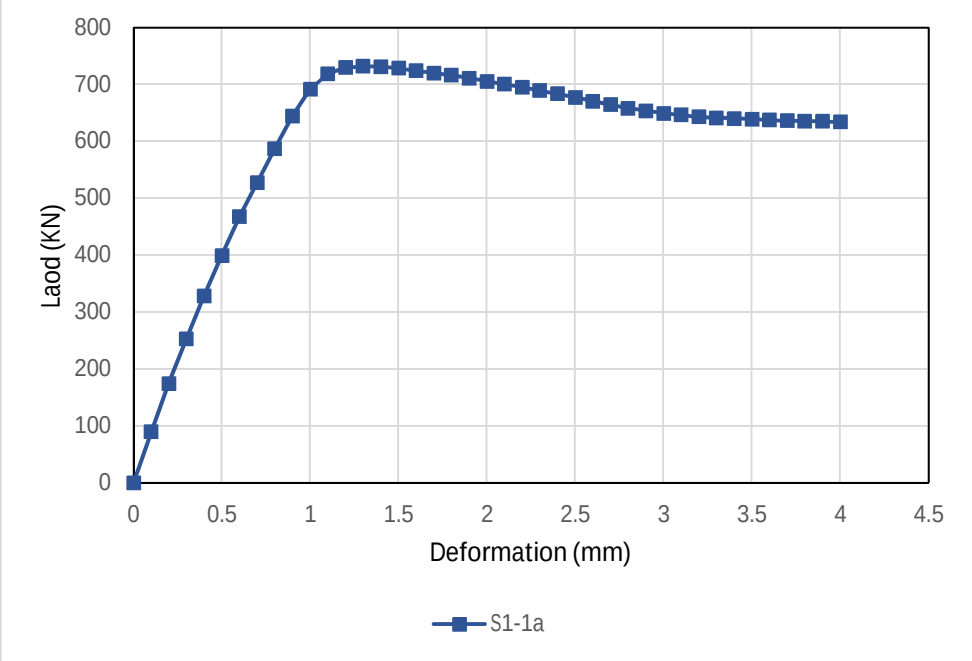

Fig.4.1 Load-deformation curve for S1-1a CFST column

4.2.2 AXIAL DEFORMATION OF S1-1b CFST COLUMN

From Fig.4.2, it can be seen that the peak load point is 1076 KN in this case. The deformation is 3mm respectively. Deformation after this point may run in an increasing pace but the load will decrease here after. As the analysis continued, the load carrying capacity decreased progressively. Further, the load has been found to be 1006 KN at the deformation of 6mm.

Table 4.2 Load and deformation values of S1-1b CFST column.

S1-1b			
Load(KN)	**Deformation(mm)**	**Load(KN)**	**Deformation(mm)**
0	0	1075	3.1
54.31	0.1	1074	3.2
108.2	0.2	1073	3.3
161.2	0.3	1072	3.4
213.2	0.4	1071	3.5
264	0.5	1070	3.6
313.6	0.6	1065	3.7
362.2	0.7	1064	3.8
410.1	0.8	1061	3.9
457.1	0.9	1058	4
503.4	1	1055	4.1
549.1	1.1	1051	4.2
594.1	1.2	1047	4.3
638.5	1.3	1043	4.4
682.4	1.4	1039	4.5
722.3	1.5	1038	4.6
764.1	1.6	1033	4.7
805.4	1.7	1031	4.8
846	1.8	1030	4.9
885.4	1.9	1028	5
919.4	2	1025	5.1
949.2	2.1	1023	5.2
975.5	2.2	1020	5.3
999	2.3	1018	5.4
1020	2.4	1015	5.5
1036	2.5	1014	5.6
1052	2.6	1012	5.7
1060	2.7	1010	5.8
1067	2.8	1008	5.9
1073	2.9	1006	6
1076	3		

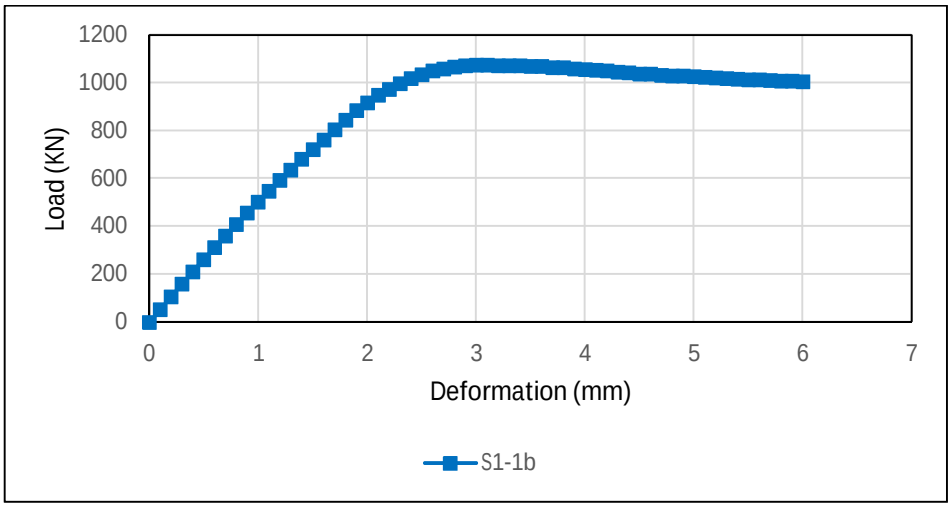

Fig. 4.2 Load-deformation curve for S1-1b CFST column

4.2.3 AXIAL DEFORMATION OF S1-2a CFST COLUMN

In the Fig.3.3, peak load point is 729.9 KN which causes deformation of 2.4mm. Deformation after this point may run in an increasing pace but the load will decrease here after. As the analysis continued, the load carrying capacity decreased progressively. Further, the load has been found to be 484.1 KN at deflection of 3.3mm.

Table 4.3 Load and deformation values of S1-2a CFST column.

S1-2a			
Load(KN)	**Deformation(mm)**	**Load(KN)**	**Deformation(mm)**
0	0	529.3	1.7
35.27	0.1	558.3	1.8
70.46	0.2	587.1	1.9
105.2	0.3	615.8	2
138.3	0.4	644.4	2.1
170.4	0.5	674	2.2
201.5	0.6	701.1	2.3
232.4	0.7	729.9	2.4
262.9	0.8	680.7	2.5
293.1	0.9	631.4	2.6
323.1	1	603.4	2.7
353	1.1	574.1	2.8
382.7	1.2	550.8	2.9
412.3	1.3	530.8	3
441.7	1.4	512.5	3.1
471	1.5	496	3.2
500.2	1.6	484.1	3.3

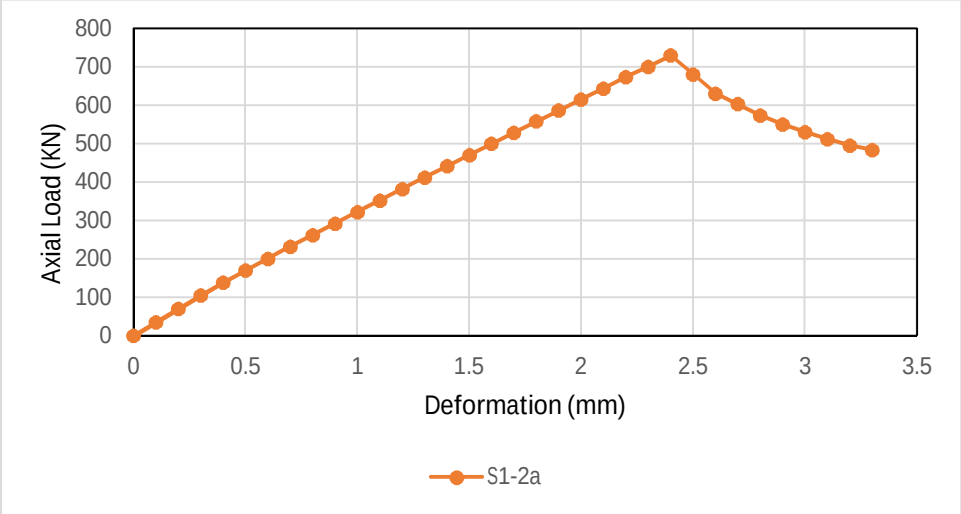

Fig. 4.3 Load-deformation curve for S1-2a CFST column

4.2.4 AXIAL DEFORMATION OF S1-2b CFST COLUMN

It is observed from Fig.4.4 that the peak load is 912 KN and the respective deformation is 2.4mm which goes on increasing upto 3mm in this model for the concerned CFST column. So this point can be taken as peak load point after which the load decreases till 684.4 KN.

Table 4.4 Load and deformation values of S1-2b CFST column.

S1-2b			
Load (KN)	**Deformation (mm)**	**Load (KN)**	**Deformation (mm)**
0	0	628.3	1.6
42.96	0.1	664.5	1.7
85.92	0.2	700.6	1.8
128.8	0.3	736.5	1.9
171.2	0.4	772.1	2
212.5	0.5	807.6	2.1
252.4	0.6	842.8	2.2
291.7	0.7	877.7	2.3
330.4	0.8	912	2.4
368.7	0.9	764.6	2.5
406.6	1	748.1	2.6
444.1	1.1	730.8	2.7
481.3	1.2	714.2	2.8
518.4	1.3	699.4	2.9
555.2	1.4	684.4	3
591.8	1.5		

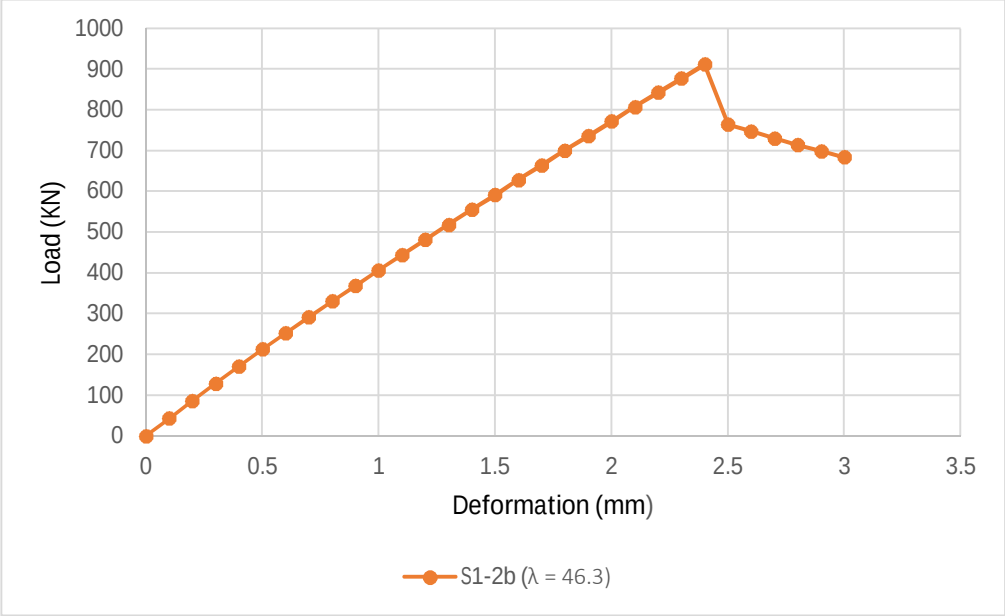

Fig. 4.4 Load-deformation curve for S1-2b CFST column

4.2.5 AXIAL DEFORMATION OF S1-3a CFST COLUMN

Fig.4.5 shows load vs. deformation graph of S1-3a. Here also no more increase of load is seen after 649.1 KN where the respective deformation is 4.1mm which has been increased upto a level of 5mm. But no more increase of load but decrease has been seen against respective deformations taken. The load carry on decreasing upto 451.9 KN.

Table 4.5 Load and deformation values of S1-3a CFST column.

S1-3a			
Load(KN)	**Deformation(mm)**	**Load(KN)**	**Deformation(mm)**
0	0	450.7	2.6
19.75	0.1	465.1	2.7
39.51	0.2	479.4	2.8
59.26	0.3	493.6	2.9
79.02	0.4	507.6	3
98.67	0.5	521.6	3.1
117.9	0.6	534.1	3.2
136.8	0.7	547.8	3.3
155.3	0.8	561.5	3.4
173.5	0.9	574.6	3.5
191.4	1	587.3	3.6
209	1.1	601.8	3.7
226.4	1.2	615.1	3.8
243.6	1.3	628.1	3.9
260.5	1.4	640.5	4
277.2	1.5	649.1	4.1
293.8	1.6	638.2	4.2

S1-3a			
Load(KN)	**Deformation(mm)**	**Load(KN)**	**Deformation(mm)**
310.2	1.7	630	4.3
326.4	1.8	610.5	4.4
342.4	1.9	580.7	4.5
358.3	2	561.8	4.6
374.1	2.1	545.7	4.7
389.7	2.2	505.3	4.8
405.2	2.3	460.9	4.9
420.6	2.4	451.9	5
435.9	2.5		

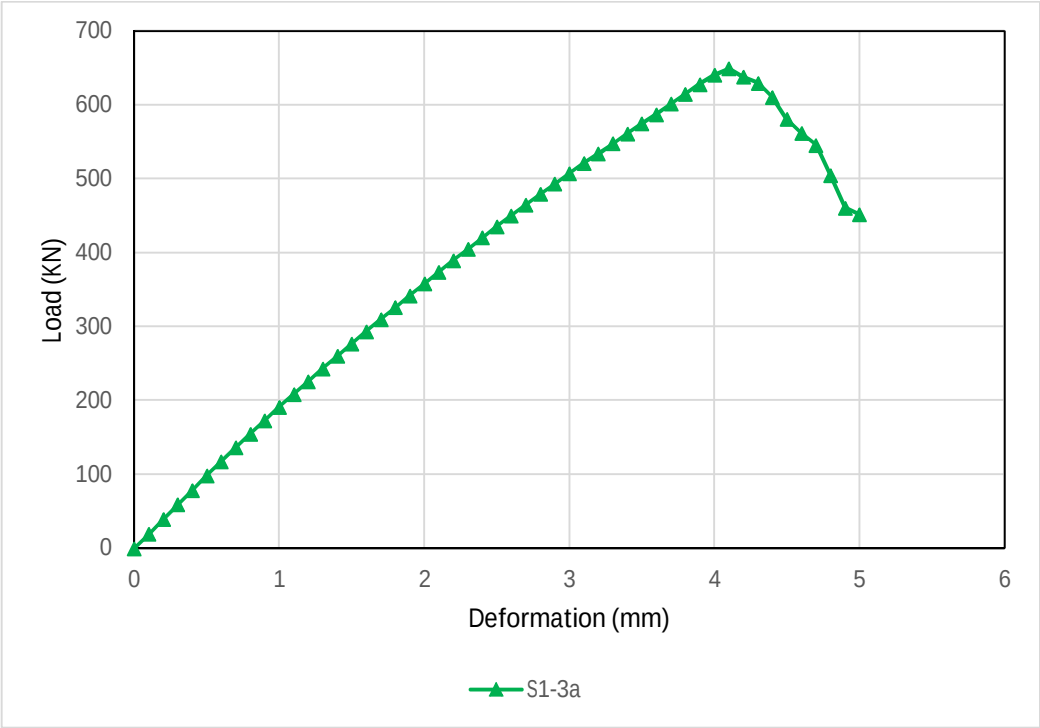

Fig. 4.5 Load-deformation curve for S1-3a CFST column

4.2.6 AXIAL DEFORMATION OF S1-3b CFST COLUMN

From Fig.4.6, it has been seen that deformation increases rapidly with the increase in load upto 703.6 KN which is the peak load for this CFST column, when deformation is 3.6mm. Subsequently deflection started increasing without any significant increment in load. As the analysis continued, the load carrying capacity decreased progressively. Further, the load has been found to be 535.3 KN at the deflection of 4.5mm.

Table 4.6. Load and deformation values of S1-3b CFST column

S1-3b			
Load (KN)	**Deformation (mm)**	**Load (KN)**	**Deformation (mm)**
0	0	489.9	2.3
23.17	0.1	507.8	2.4
46.33	0.2	525.6	2.5
69.5	0.3	543.2	2.6
92.66	0.4	560.7	2.7
115.8	0.5	578.1	2.8
139	0.6	594.2	2.9
162	0.7	611.3	3
184.6	0.8	628.2	3.1
206.9	0.9	644.6	3.2
228.8	1	661.5	3.3
250.4	1.1	678	3.4
271.7	1.2	693.6	3.5
292.7	1.3	703.6	3.6
313.5	1.4	654.3	3.7
334	1.5	621	3.8
354.3	1.6	600	3.9
374.4	1.7	584.3	4
394.3	1.8	572.2	4.1
414	1.9	561.4	4.2
433.5	2	552	4.3
452.8	2.1	543.3	4.4
471.6	2.2	535.3	4.5

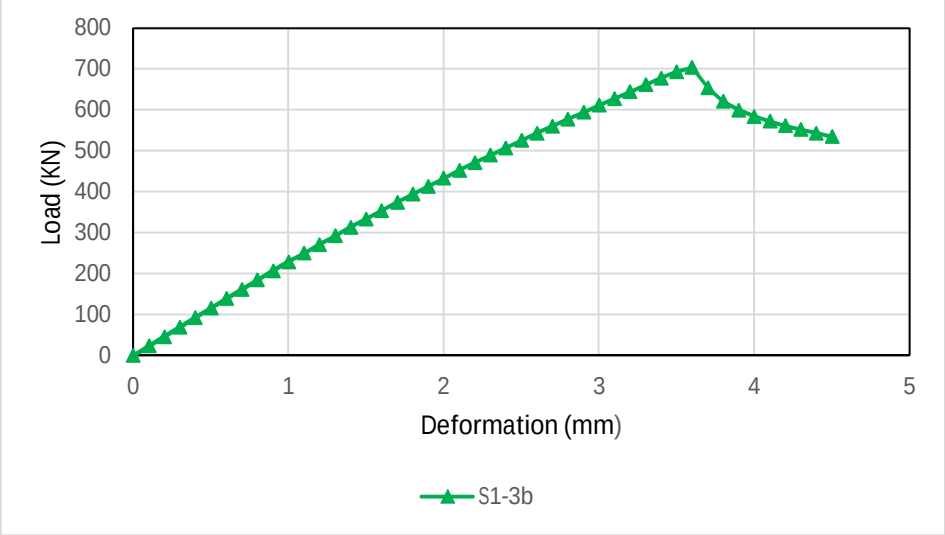

Fig.4.6 Load-deformation curve for S1-3b CFST column

4.3 MID HEIGHT DEFLECTION OF CFST COLUMN UNDER AXIAL LOADING

After studying the axial deformation behaviour of CFST column, mid height deflection behaviour is carried out. Mid-point of the column along the length is monitored to obtain the mid-height deflection.

4.3.1 MID HEIGHT DEFLECTION OF S1-1a CFST COLUMN

In Fig.4.7, x- axis represents mid-height deflection in mm and y-axis describes axial load in KN. It has been seen that mid-height deflection increases rapidly with the increase in axial load upto 732.5 KN which is the peak load for this CFST column, when deflection is 0.395mm. The deflection keeps on increasing even after this point but the load starts decreasing accordingly. As the analysis continued, the load carrying capacity decreased progressively. Further, the axial load has been found to be 634.6 KN at the deflection of 1.073mm.

Table 4.7. Load and deflection values of S1-1a CFST column.

S1-1a		**S1-1a**	
Load (KN)	**Mid-height deflection (mm)**	**Load (KN)**	**Mid-height deflection (mm)**
0	0	700.9	0.5995
90.38	0.036	695.5	0.6278
174.9	0.0732	689.5	0.6554
253.8	0.10955	683.8	0.6813
328.5	0.1455	678	0.7038
400	0.1815	671.2	0.7236
468.5	0.2173	665.1	0.7434
527.5	0.2521	658.7	0.7629
587.6	0.2863	654	0.7841
644.6	0.3197	649.6	0.8061
692.1	0.3504	647.1	0.8302
719.3	0.3694	643.6	0.8539
729.8	0.3801	641.7	0.8781
732.5	0.3955	640.7	0.9057
731.5	0.4154	639.4	0.9325
729	0.4387	637.9	0.9596
724.7	0.4633	636.7	0.9871
720.7	0.4896	636.1	1.015
716.5	0.5169	635.5	1.044
711.8	0.5446	634.6	1.073
706.1	0.5717		

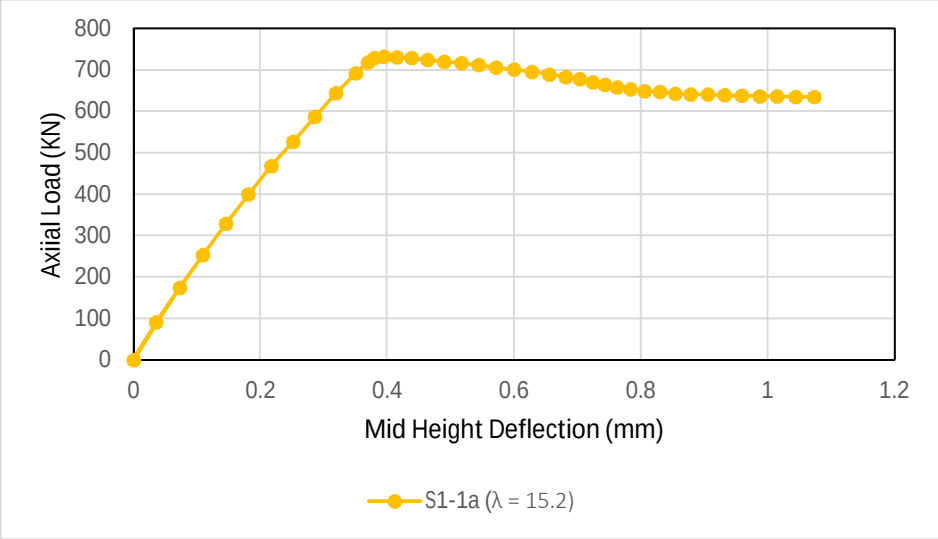

Fig.4.7 Axial load vs. mid-height deflection curve for S1-1a CFST column.

4.3.2 MID HEIGHT DEFLECTION OF S1-1b CFST COLUMN

From Fig.4.8, it can be seen that the peak load point is 1076 KN in this case. The deflection is 0.341mm respectively. Deflection after this point may run in an increasing pace but the load will decrease here after. As the analysis continued, the axial load carrying capacity decreased progressively. Further, the axial load has been found to be 1006 KN at the deflection of 1.412mm.

Table 4.8 Load and deflection values of S1-1b CFST column.

S1-1b			
Load (KN)	**Mid height deflection (mm)**	**Load (KN)**	**Mid height deflection (mm)**
0	0	1075	0.356
54.31	0.018	1074	0.37
108.2	0.026	1073	0.39
161.2	0.034	1072	0.421
213.2	0.045	1071	0.433
264	0.054	1070	0.461
313.6	0.072	1065	0.482
362.2	0.084	1064	0.498
410.1	0.093	1061	0.521
457.1	0.098	1058	0.534
503.4	0.102	1055	0.56
549.1	0.114	1051	0.582
594.1	0.126	1047	0.61
638.5	0.138	1043	0.63
682.4	0.147	1039	0.65

S1-1b			
Load (KN)	**Mid height deflection (mm)**	**Load (KN)**	**Mid height deflection (mm)**
722.3	0.156	1038	0.674
764.1	0.163	1033	0.7
805.4	0.177	1031	0.742
846	0.189	1030	0.78
885.4	0.197	1028	0.82
919.4	0.208	1025	0.865
949.2	0.216	1023	0.892
975.5	0.223	1020	0.941
999	0.239	1018	0.982
1020	0.248	1015	1.01
1036	0.254	1014	1.064
1052	0.267	1012	1.152
1060	0.278	1010	1.276
1067	0.285	1008	1.367
1073	0.32	1006	1.412
1076	0.341		

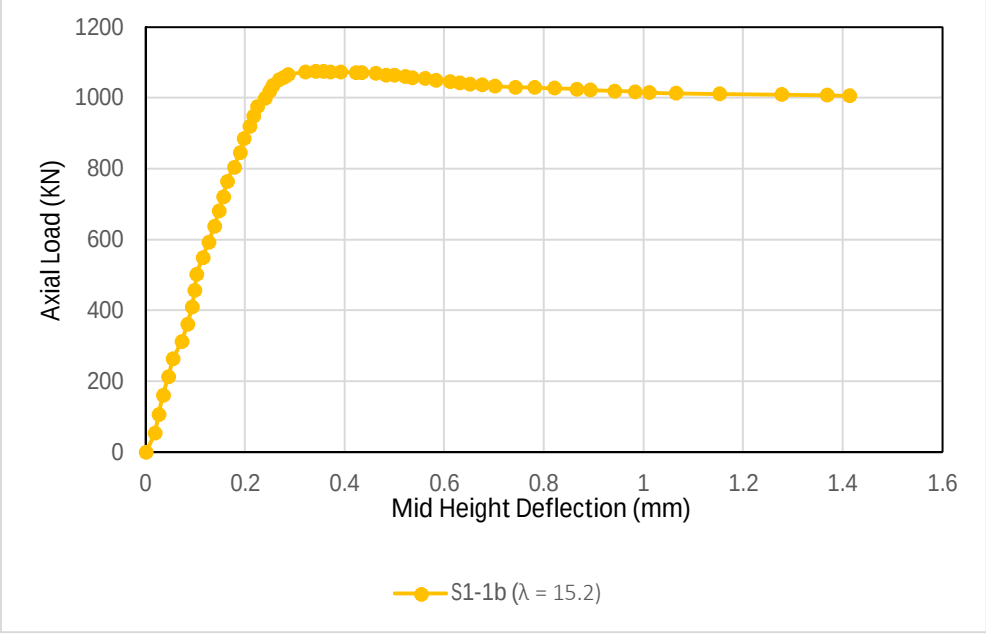

Fig.4.8 Axial load vs. mid-height deflection curve for S1-1b CFST column.

4.3.3 MID HEIGHT DEFLECTION OF S1-2a CFST COLUMN

In the Fig.3.3, peak load point is 729.9 KN which causes deflection of 2.122mm. Deflection after this point may run in an increasing pace but the load will decrease here after. As the analysis continued, the axial load carrying capacity decreased progressively. Further, the load has been found to be 484.1 KN at deflection of 2.9mm.

Table 4.9 Load and deflection values of S1-2a CFST column.

S1-2a			
Load (KN)	**Mid height deflection (mm)**	**Load (KN)**	**Mid height deflection (mm)**
0	0	529.3	1.516
35.27	0.124	558.3	1.603
70.46	0.211	587.1	1.69
105.2	0.298	615.8	1.778
138.3	0.385	644.4	1.865
170.4	0.472	674	1.952
201.5	0.559	701.1	2.038
232.4	0.646	729.9	2.122
262.9	0.733	680.7	2.209
293.1	0.82	631.4	2.296
323.1	0.907	603.4	2.383
353	0.994	574.1	2.47
382.7	1.081	550.8	2.557
412.3	1.168	530.8	2.644
441.7	1.255	512.5	2.731
471	1.342	496	2.818
500.2	1.429	484.1	2.9

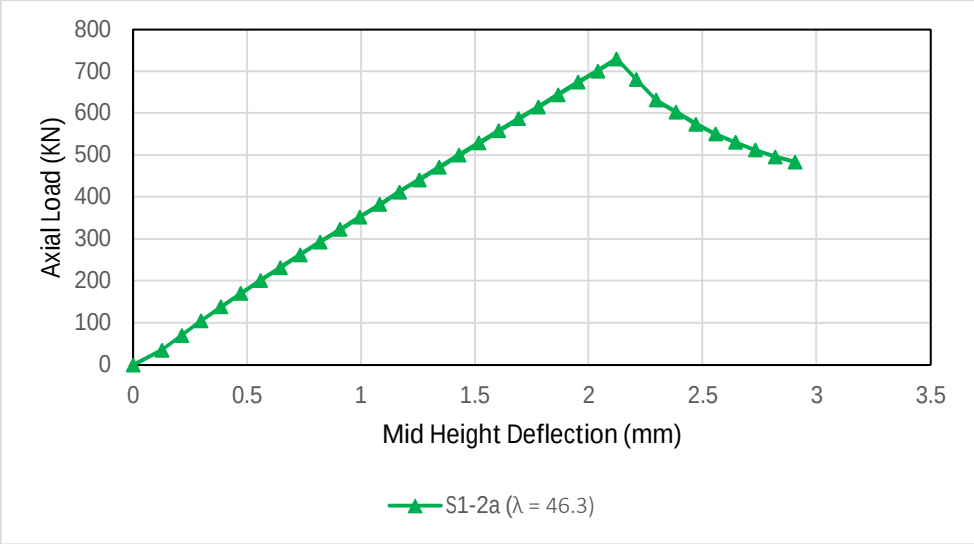

Fig.4.9 Axial load vs. mid-height deflection curve for S1-2a CFST column.

4.3.4 MID HEIGHT DEFLECTION OF S1-2b CFST COLUMN

It is observed from Fig.4.10 that the peak load is 912 KN and the respective deflection is 1.123mm which goes on increasing upto 2.842mm in this model for the concerned CFST column. So this point can be taken as peak load point after which the axial load decreases till 684.4 KN.

Table 4.10 Load and deflection values of S1-2b CFST column.

S1-2b			
Load (KN)	**Mid height deflection (mm)**	**Load (KN)**	**Mid height deflection (mm)**
0	0	628.3	0.736
42.96	0.0459	664.5	0.783
85.92	0.0919	700.6	0.83
128.8	0.1379	736.5	0.877
171.2	0.1838	772.1	0.924
212.5	0.229	807.6	0.971
252.4	0.275	842.8	1.02
291.7	0.321	877.7	1.07
330.4	0.367	912	1.123
368.7	0.413	764.6	2.007
406.6	0.459	748.1	2.206
444.1	0.505	730.8	2.388
481.3	0.551	714.2	2.551
518.4	0.597	699.4	2.701
555.2	0.644	684.4	2.842
591.8	0.69		

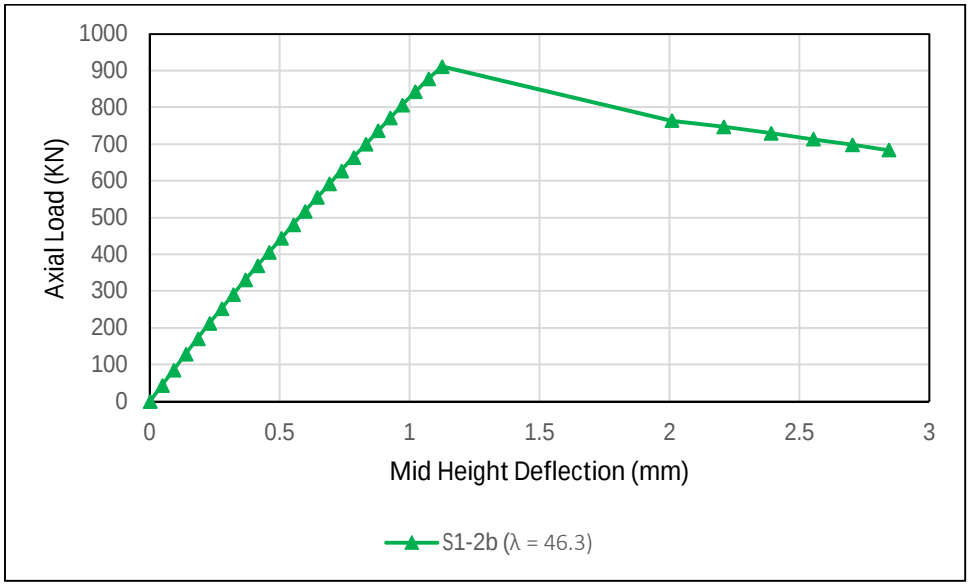

Fig.4.10 Axial load vs. mid-height deflection curve for S1-2b CFST column.

4.3.5 MID HEIGHT DEFLECTION OF S1-3a CFST COLUMN

Fig.4.11 shows axial load vs. mid-height deflection graph of S1-3a. Here also no more increase of axial load is seen after 649.1 KN where the respective deflection is 4.23mm which has been increased upto a level of 5.24mm. But no more increase of load but decrease has been seen against respective deformations taken. The load carry on decreasing upto 451.9 KN.

Table 4.11 Load and deflection values of S1-3a CFST column.

S1-3a			
Load (KN)	**Mid height deflection (mm)**	**Load (KN)**	**Mid height deflection (mm)**
0	0	450.7	2.66
19.75	0.123	465.1	2.75
39.51	0.241	479.4	2.83
59.26	0.355	493.6	2.94
79.02	0.442	507.6	3.03
98.67	0.562	521.6	3.16
117.9	0.643	534.1	3.25
136.8	0.764	547.8	3.35
155.3	0.839	561.5	3.42
173.5	0.941	574.6	3.53
191.4	1.06	587.3	3.61
209	1.15	601.8	3.7
226.4	1.26	615.1	3.82
243.6	1.37	628.1	3.94
260.5	1.45	640.5	4.13
277.2	1.54	649.1	4.23
293.8	1.63	638.2	4.35
310.2	1.77	630	4.46
326.4	1.84	610.5	4.53
342.4	1.95	580.7	4.62
358.3	2.04	561.8	4.72
374.1	2.16	545.7	4.85
389.7	2.24	505.3	4.96
405.2	2.35	460.9	5.13
420.6	2.44	451.9	5.24
435.9	2.57		

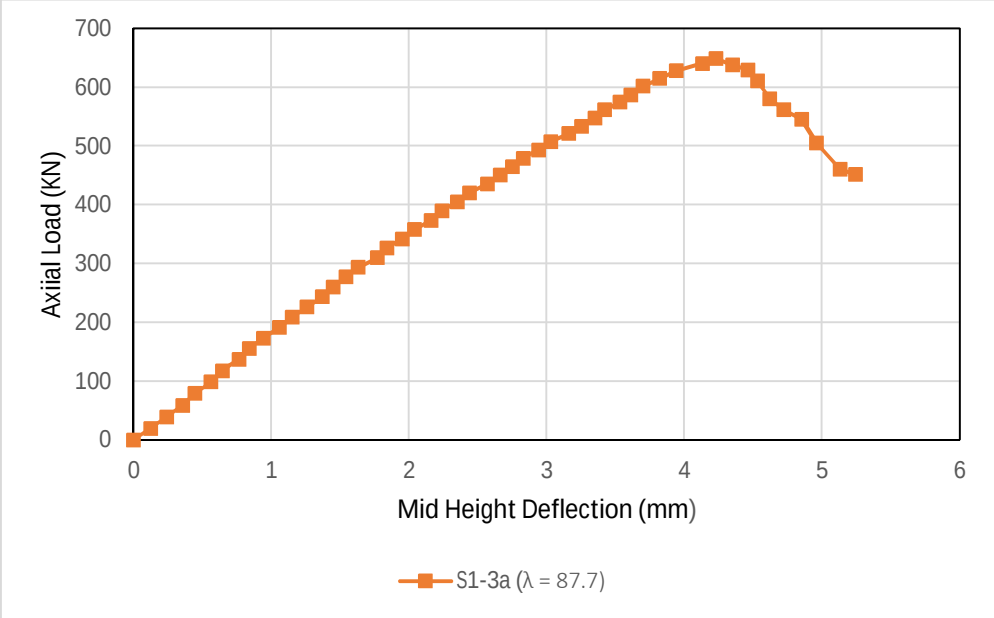

Fig.4.11 Axial load vs. mid-height deflection curve for S1-3a CFST column.

4.3.6 MID HEIGHT DEFLECTION OF S1-3b CFST COLUMN

From Fig.4.12, it has been seen that deformation increases rapidly with the increase in load upto 703.6 KN which is the peak load for this CFST column, when deformation is 3.78mm. Subsequently deflection started increasing without any significant increment in load. As the analysis continued, the load carrying capacity decreased progressively. Further, the load has been found to be 535.3 KN at the deflection of 4.81mm.

Table 4.12 Load and deflection values of S1-3b CFST column.

S1-3b			
Load (KN)	**Mid height deflection (mm)**	**Load (KN)**	**Mid height deflection (mm)**
0	0	489.9	2.34
23.17	0.13	507.8	2.46
46.33	0.24	525.6	2.58
69.5	0.35	543.2	2.67
92.66	0.438	560.7	2.74
115.8	0.54	578.1	2.89
139	0.67	594.2	2.98
162	0.78	611.3	3.04
184.6	0.88	628.2	3.18
206.9	0.96	644.6	3.3
228.8	1.08	661.5	3.42
250.4	1.13	678	3.52
271.7	1.27	693.6	3.64

S1-3b			
Load (KN)	**Mid height deflection (mm)**	**Load (KN)**	**Mid height deflection (mm)**
292.7	1.36	703.6	3.78
313.5	1.45	654.3	3.89
334	1.56	621	3.99
354.3	1.63	600	4.04
374.4	1.78	584.3	4.16
394.3	1.84	572.2	4.28
414	1.92	561.4	4.41
433.5	2	552	4.58
452.8	2.13	543.3	4.7
471.6	2.28	535.3	4.81

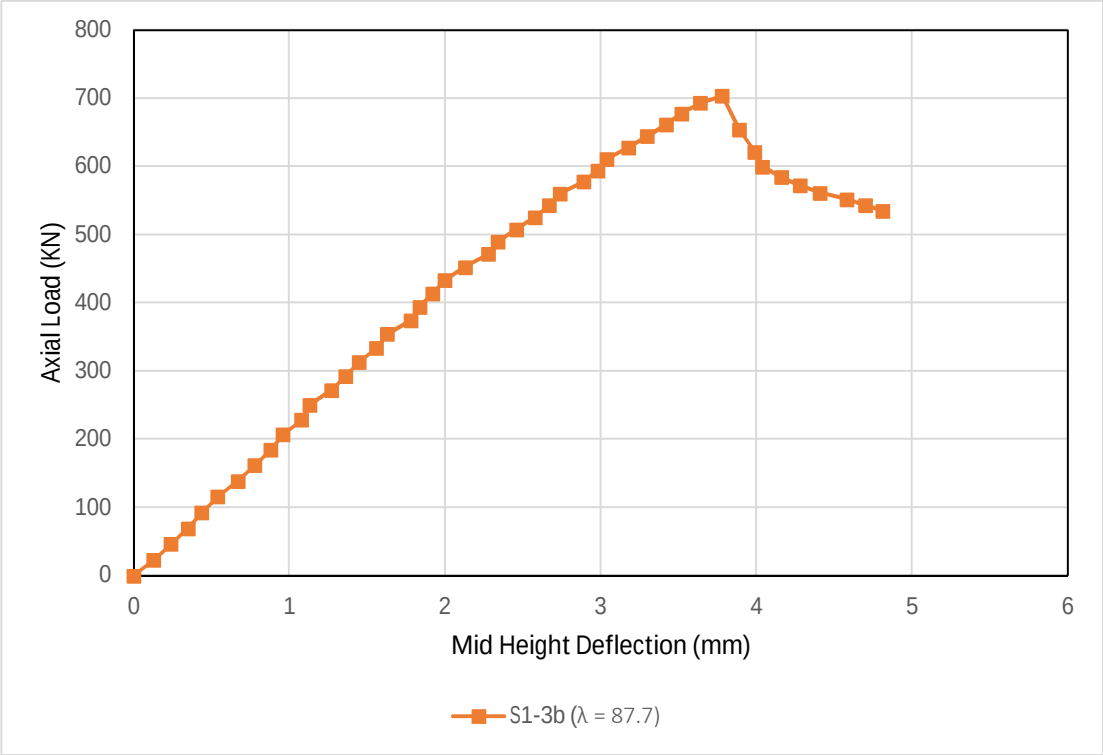

Fig.4.12 Axial load vs. mid-height deflection curve for S1-3a CFST column.

4.4 COMPARISON BETWEEN EXPERIMENTAL RESULTS AND FEM RESULTS OF CFST COLUMN UNDER AXIAL LOADING

After studied the behaviour of all CFST columns under axial loading, results of analytical modelling are compared with experimental results of CSFT column under axial loading.

4.4.1 COMPARISON BETWEEN EXPERIMENTAL AND FEM RESULTS OF THE SPECIMENS HAVING CYLINDRICAL COMPRESSIVE STRENGTH OF 36.3 MPa.

All the experimental and analytical results have been compared carefully. Table 4.13 shows comparison of experimental and FEM results. Fig.4.7 and Fig. 4.8 shows the curve for load vs. mid height deflection of FEM and experimental results respectively. λ is the slenderness ratio. As seen from both of the graphs that larger the slenderness ratio smaller the peak load is. In S1-1a specimen, experimental value of peak load is 767.6 KN at 0.33mm deflection. Where FEM value of peak load is 732.5 KN at 0.395mm deflection. Hence peak load and deflection values of both the results have almost similar values. In S1-2a specimen, experimental value of peak load is 697.3 KN at 2.65 mm deflection. Where analytical value of peak load is 729.9 KN at 2.122mm. Peak loads of both the results have almost similar values and also the value of deflection of both the results match well. In S1-3a specimen, experimental value of peak load is 622.9 KN at 4.42mm deflection. Where analytical value of peak load is 649.1 KN at 4.23mm. Here also peak loads of both the results have almost similar values and also value of deflection of both the results match well.

As seen from the above discussion that after the peak load point, deflection increases even when load tends to decrease. Fig.4.14 shows experimental values which indicates decrease in load after the peak load point and the deflection gradually increases upto 15mm, 30mm and 60 mm approximately for S1-1a, S1-2a and S1-3a respectively. However, Fig.4.13 shows the FEM results which indicates that after the peak load point, the deflection increases upto 1.073mm, 2.9mm and 5.24mm for S1-1a, S1-2a and S1-3a respectively, where load tends to decrease. Deformation steps are taken upto the certain points so that peak load is achieved. Step size of the deformation is 0.1mm. Due to these deformation steps, peak load is achieved and consequently deflection is obtained at the mid-point. It is very time consuming to achieve the deflection of 15mm,

30mm and 60mm approximately for S1-1a, S1-2a and S1-3a respectively as taken in experiment because there are several steps for these deformations at increment of 0.1mm. Hence only certain deformation steps are taken to achieve the peak load and also to obtain the deflection.

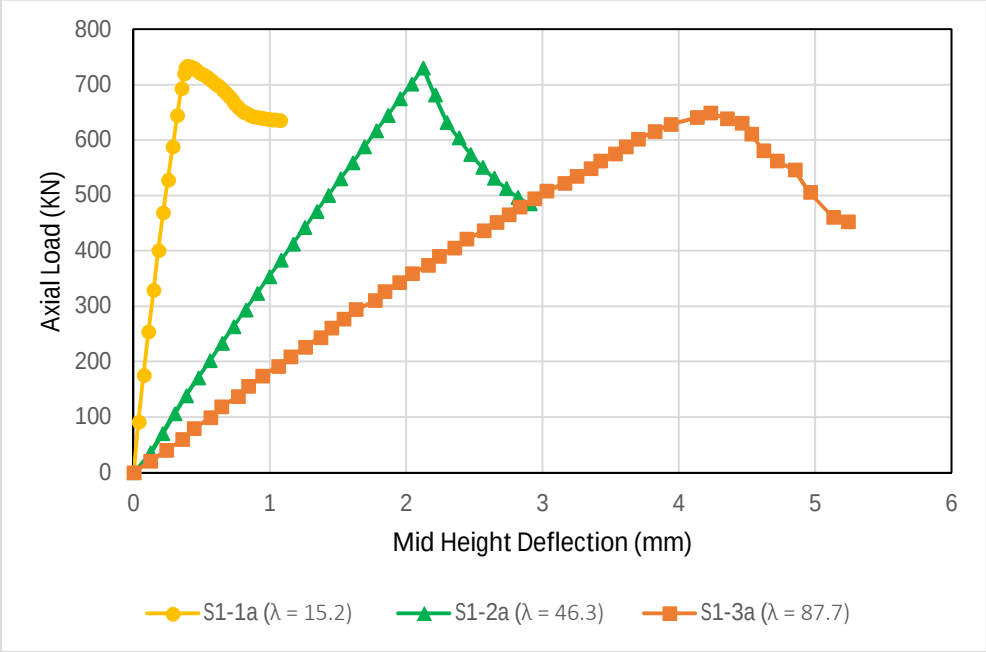

Fig.4.13 Load-deflection combined curve (FEM) of S1-1a, S1-2a and S1-3a.

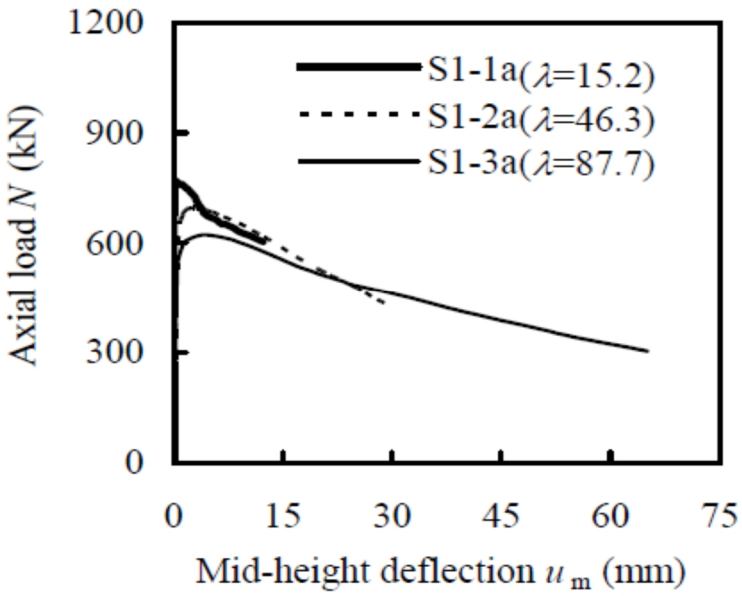

Fig.4.14 Load-deflection combined curve (Experimental) of S1-1a, S1-2a and S1-3a. [25]

Table 4.13 Comparison of experimental and FEM results.

No.	Specimen Label	Peak Load (Experimental) (KN)	Mid Height Deflection (Experimental) (mm)	Peak Load (FEM) (KN)	Mid-Height Deflection (FEM) (mm)
1	S1-1a	767.6	0.33	732.5	0.395
2	S1-1b	1090.5	0.29	1076	0.341
3	S1-2a	697.3	2.65	729.9	2.122
4	S1-2b	1022.9	0.83	912	1.123
5	S1-3a	622.9	4.42	649.1	4.230
6	S1-3b	684.2	10.82	703.6	3.78

4.4.2 COMPARISON BETWEEN EXPERIMENTAL AND FEM RESULTS OF THE SPECIMENS HAVING CYLINDRICAL COMPRESSIVE STRENGTH OF 75.4 MPa.

All the experimental and analytical results have been compared carefully. Fig.4.15 and Fig. 4.16 shows the curve for load vs. mid-height deflection of FEM and experimental results respectively. Here also peak load decreases as slenderness ratio increases. In S1-1b specimen, experimental value of peak load is 1090.5 KN at 0.29mm deflection. Where analytical value of peak load is 1076 KN at 0.341mm. Peak load and deflection values of both the results have almost similar values. In S1-2b specimen, experimental value of peak load is 1022.9 KN at 0.83mm deflection. Where analytical value of peak load is 912 KN at 1.123mm. Peak loads of both the results have almost similar values and also the value of deflection of both the results match well. In S1-3b specimen, experimental value of peak load is 684.2 KN at 10.82mm deflection. Where analytical value of peak load is 703.6 KN at 3.78mm. Although peak loads of both the results have almost similar values, but the value of deflection of both the results do not match.

As seen from the above discussion that after the peak load point deflection increases even when load tends to decrease. Fig.4.16 shows experimental values which indicates decrease in load after the peak load point and the deflection gradually increases upto 11mm, 30mm and 65 mm approximately for S1-1b, S1-2b and S1-3b respectively. However, Fig.4.15 shows that FEM results which indicates that after the peak load point, deflection increases upto 1.412mm, 2.842mm and 4.81mm for S1-1b, S1-2b and S1-3b respectively, where load tends to decrease. Deformation steps are taken upto the

certain points so that peak load is achieved. Step size of the deformation is 0.1mm. Due to these deformation steps, peak load is achieved and consequently deflection is obtained at the mid-point. It is very time consuming to achieve the deformation of 11mm, 30mm and 65mm approximately for S1-1b, S1-2b and S1-3b respectively as taken in experiment because there are several steps for these deformations at increment of 0.1mm. Hence, only certain deformation steps are taken to achieve the peak load and also to obtain deflection at mid-point.

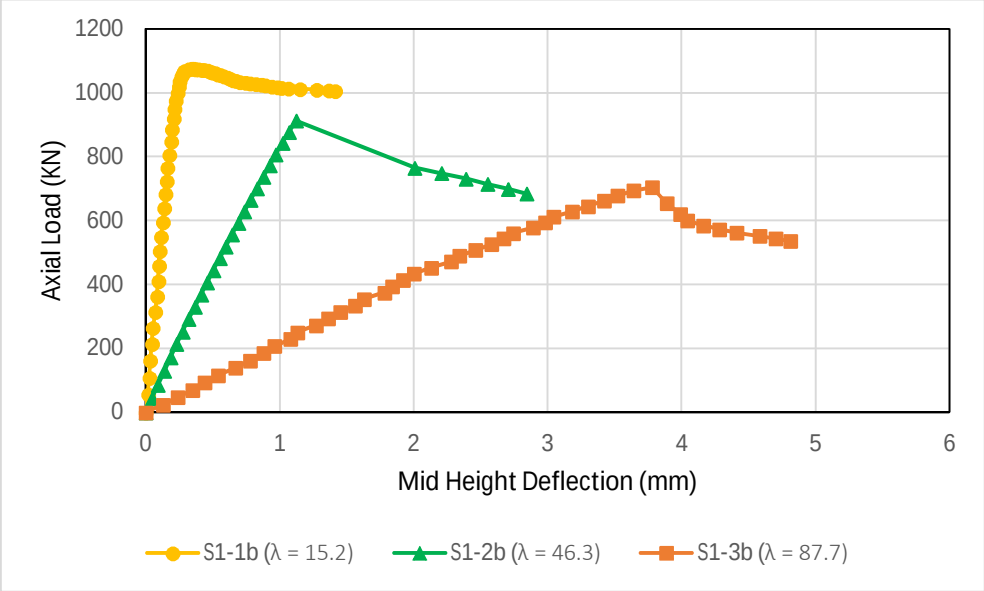

Fig.4.15 Load-deflection combined curve (FEM) of S1-1b, S1-2b and S1-3b

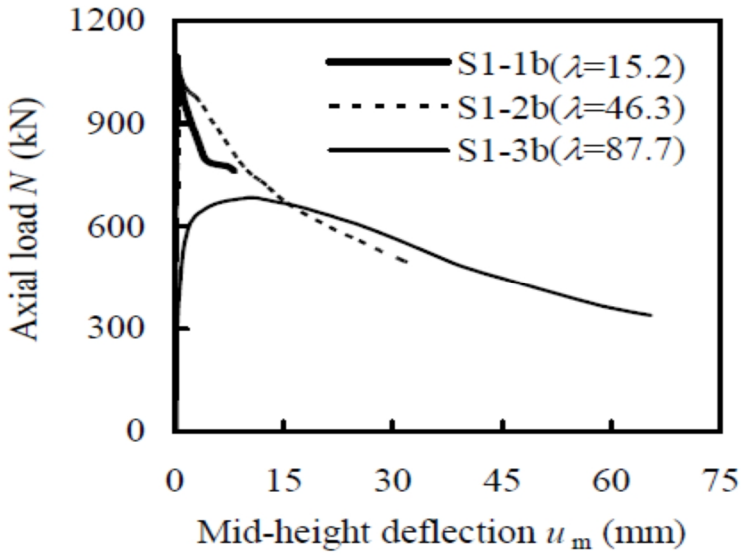

Fig.4.16 Load-deflection combined curve(Experimental) of S1-1b,S1-2b and S1-3b. [25]

4.4.3 COMPARISON BETWEEN EXPERIMENTAL AND FE RESULTS OF THE SPECIMENS S1-1a AND S1-1b

From Fig.4.17 and Fig.4.18, S1-1a specimen, experimental value of peak load is 767.6 KN at 0.33mm deflection. Where analytical value of peak load is 732.5 KN at 0.395mm. Peak load and deflection values of both the results have almost similar values. In S1-1b specimen, experimental value of peak load is 1090.5 KN at 0.29mm deflection. Where analytical value of peak load is 1076 KN at 0.341mm deflection. Hence peak loads of both the results have almost similar values and the values of deflection of both the results match well.

As seen from the above discussion that after the peak load point deflection increases even when load tends to decrease. Fig.4.18 shows experimental values which indicates decrease in load after the peak load point and the deflection gradually increases upto 9mm and 12mm approximately for S1-1a and S1-1b respectively. However, Fig.4.17 shows the FEM results which indicates that after the peak load point, the deflection increases upto 1.073mm and 1.412mm for S1-1a and S1-1b respectively, where load tends to decrease. Deformation steps are taken upto the certain points so that peak load is achieved. Step size of the deformation is 0.1mm. It is very time consuming to achieve the deformation of 9mm and 12mm for S1-1a and S1-1b respectively as taken in experiment because there are several steps for this deformation at increment of 0.1mm. Hence only certain deformation steps are taken to achieve the peak load and also to obtain the deflection at mid-point.

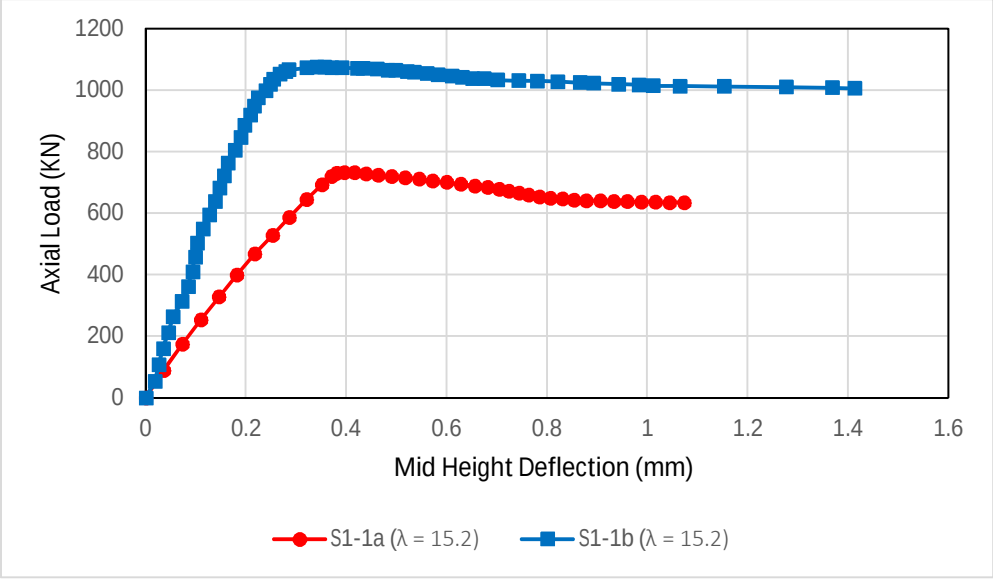

Fig.4.17 Load-deflection combined curve (FEM) of S1-1a and S1-1b

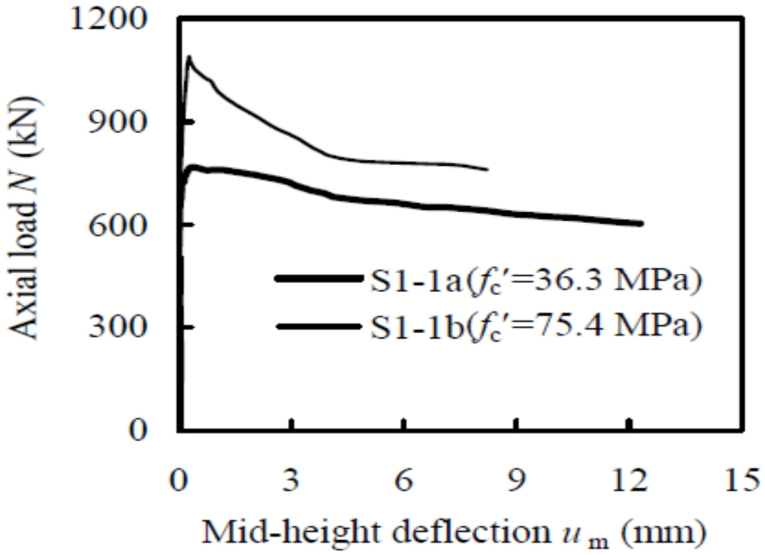

Fig.4.18 Load-deflection combined curve (Experimental) of S1-1a and S1-1b. [25]

4.4.4 COMPARISON BETWEEN EXPERIMENTAL AND FE RESULTS OF THE SPECIMENS S1-3a AND S1-3b

From Fig.4.19 and Fig.4.20, S1-3a specimen, experimental value of peak load is 622.9 KN at 4.42mm deflection. Where analytical value of peak load is 649.1 KN at 4.23mm. Here, peak loads of both the results have almost similar values and also values of deflection of both the results match well. In S1-3b specimen, experimental value of peak load is 684.2 KN at 10.82mm deflection. Where analytical value of peak load is 703.6 KN at 3.78mm. Although peak loads of both the results have almost similar values, but the values of deflection of both the results do not match.

As seen from the above discussion that after the peak load point deflection increases even when load tends to decrease. Fig.4.20 shows experimental values which indicates decrease in load after the peak load point and the deflection gradually increases upto 60mm approximately for both S1-3a and S1-3b respectively. However, Fig.4.19 shows the FEM results which indicates that after the peak load point, deflection increases upto 5.24mm and 4.81mm for S1-3a and S1-3b respectively, where load tends to decrease. Deformation steps are taken upto the certain points so that peak load is achieved. Step size of the deformation is 0.1mm. It is very time consuming to achieve the deformation of 60mm approximately for both S1-3a and S1-3b respectively as taken in experiment because there are several steps for this deformation at increment of 0.1mm. Hence only

certain deformation steps are taken to achieve the peak load and also to obtain deflection at mid-point.

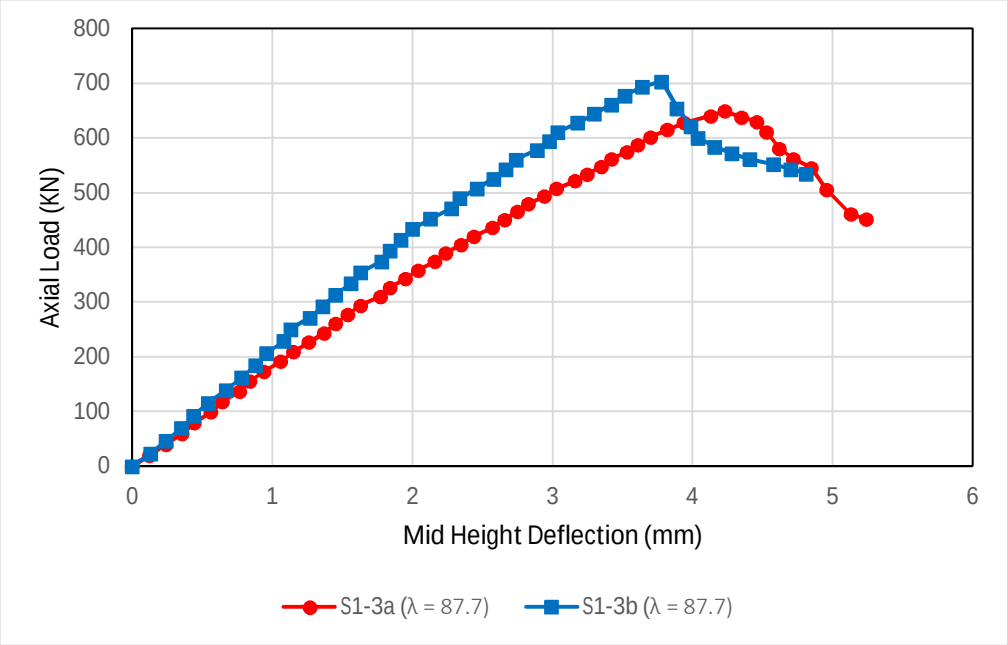

Fig.4.19 Load-deflection combined curve (FEM) of S1-3a and S1-3b.

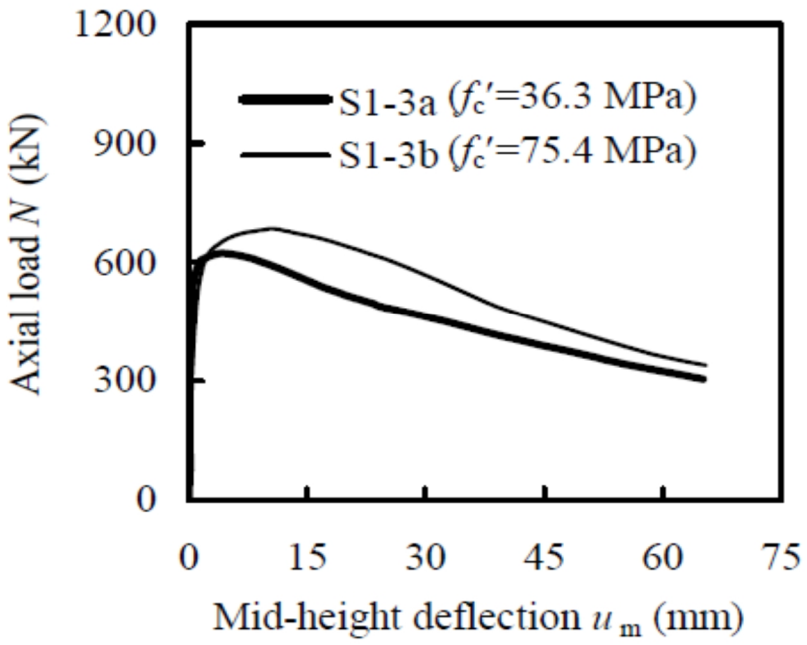

Fig.4.20 Load-deflection combined curve (Experimental) of S1-3a and S1-3b. [25]

4.5 STUDY OF PREVIOUS RESEARCH WORK (Schneider, 1998) TO RECTIFY MISLEADING DATA OF THE CURRENT RESEARCH

In current study it has been found that some results are not very satisfactory. Hence, to check this, another research paper (Schneider, 1998) has been taken account. Schneider presented experimental and analytical study on behaviour of axially loaded concrete filled steel tubes. Fourteen specimens were tested. Among them three were circular, five square and six rectangular. As the current study has been done on square concrete filled steel tubular columns, only the results of square columns have been taken into account. Table 4.14 represents Schneider's work on square concrete filled steel tubular columns whereas Table 4.15 stands for current study data.

Table 4.14 Results from Schneider's study. [21]

Sample	**Length (mm)**	**Size (B x t) mm**	**E_s (MPa)**	**E_c (MPa)**	**f_c (MPa)**	**F_y (MPa)**	**Peak Load (KN)**
S1	635	127 x 3.15	180518	26611	30.45	356	868
S2	635	127 x 4.34	190164	24609	26.04	357	1024
S3	635	127 x 4.55	205322	23528	23.8	322	1090
S4	635	127 x 5.67	203944	23528	23.8	312	1179
S5	635	127 x 7.47	204633	23528	23.8	347	1647

Table 4.15 Results of current study.

Sample	**Size (B x t)**	**L (mm)**	**f_c (MPa)**	**E_s (MPa)**	**E_c (MPa)**	**σ_y(MPa) (yield stress)**	**Peak Load (FEM) (KN)**
S1-1a	100.3 x 2.76	440	36.3	210000	33900	390.3	732.5
S1-1b	100.3 x 2.76	440	75.4	210000	37900	390.3	1076
S1-2a	100.3 x 2.76	1340	36.3	210000	33900	390.3	729.9
S1-2b	100.3 x 2.76	1340	75.4	210000	37900	390.3	894.8
S1-3a	100.3 x 2.76	2540	36.3	210000	33900	390.3	649.1
S1-3b	100.3 x 2.76	2540	75.4	210000	37900	390.3	703.6

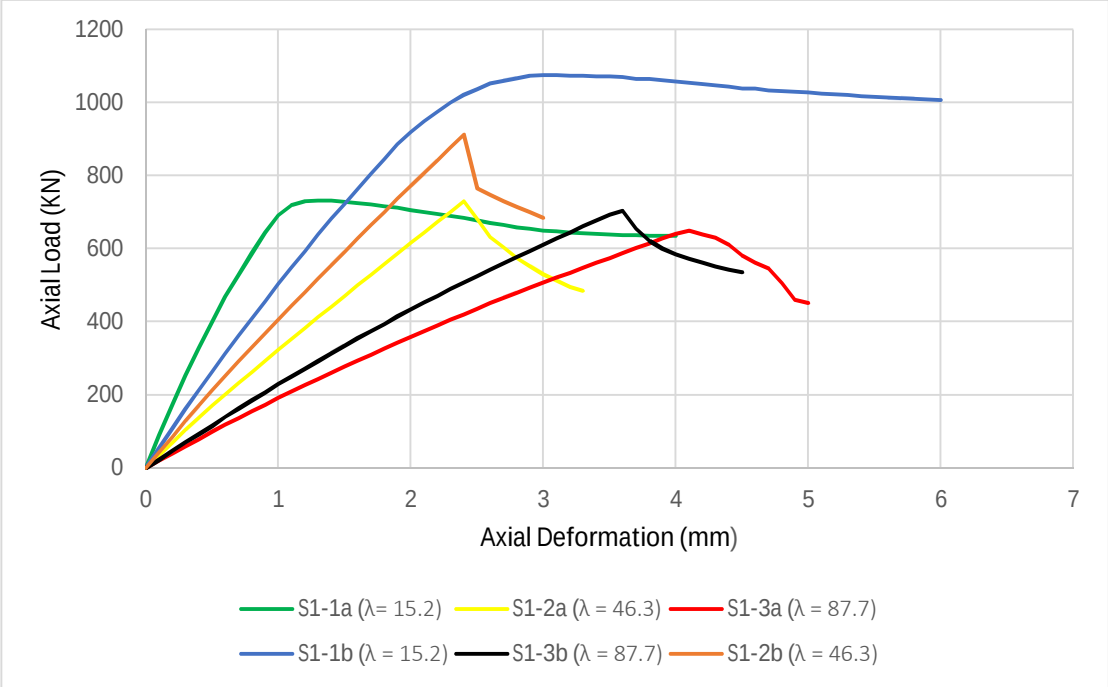

Fig. 4.21 Load vs. axial deformation curve of current study.

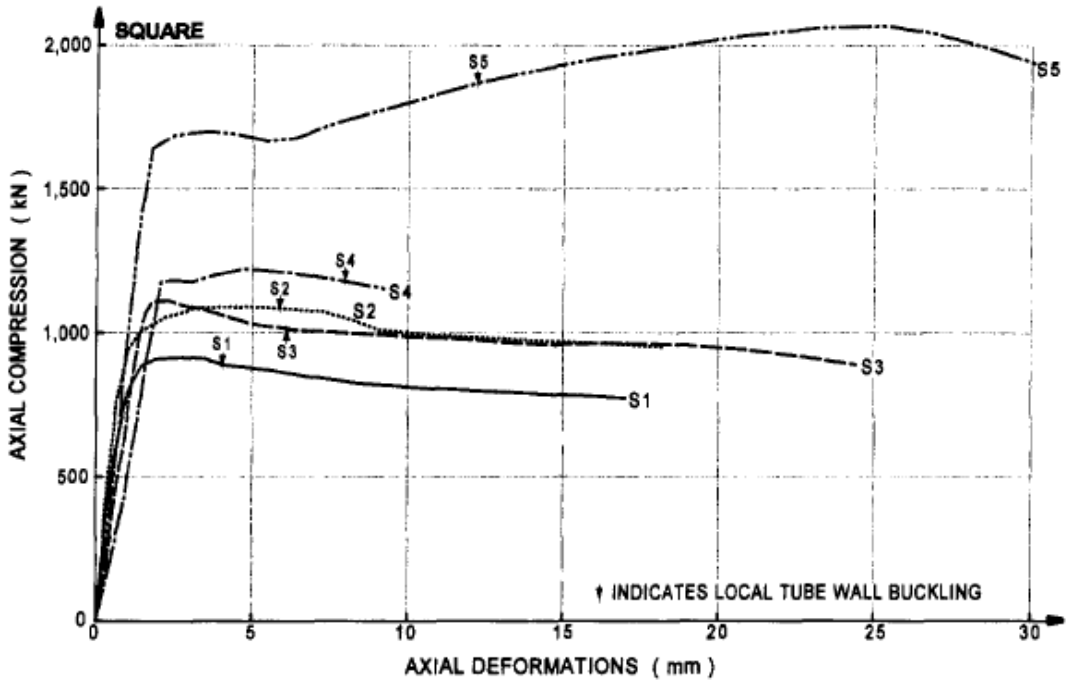

Fig.4.22 Load vs. axial deformation curve of Schneider's study. [21]

In Fig.4.21 it is clear that deformation steps are taken upto the certain points. Once peak load is achieved, load gradually decreases with further increase in deformation. Hence steps are taken upto certain points where peak load is achieved.

Both the above graphs i.e. Fig.4.21 and Fig.4.22 represents load vs. deformation of CFST column. The deformations in Schneider's study varied from 1mm to 4.5mm approximately for the peak loads 868 KN to 1647 KN respectively. In the current study, deformations varied from 1.3mm to 4.1mm for peak loads 649.1 KN to 1076 KN respectively. Similar trend is observed on both the graphs. Although in Schneider's study different values of thickness, characteristic compressive strength of concrete and yield stress of steel have been found, in current study too different length and characteristic compressive strength have been found. As a result both of them yield similar kind of graph pattern upto peak load.

Finally, this comparative study confirms that current study leading to unsatisfactory result are not completely incorrect. The mismatched result may be a cause of some different conditions taken during experimental and analytical work.

CHAPTER 5 CONCLUSIONS AND RECOMMENDATIONS

5.1 GENERAL

In the present study, the non-linear response of concrete filled steel tubular columns under axial loading has been found out with the intention to study the relative importance of several factors in the non-linear finite element analysis of concrete filled steel tubular columns.

5.2 CONCLUSIONS

The main observations from the analysis are summarized below:

(1) The value of FEM peak loads are closer to experimental peak loads of all the specimens of concrete filled steel tubular columns.

(2) The deflections at peak loads of both experimental and FEM results are almost same in case of S1-1a, S1-1b, S1-2a, S1-2b and S1-3b. Hence these specimens shows good resemblance. Only S1-3b shows mismatched result.

(3) As two compressive strengths of concrete are taken in account for three specimens of different dimension. Hence six specimens are categorized. It was found that higher the compressive strength of concrete in the specimen smaller will be the deflection.

(4) Stainless steel is used for the steel tube in CSFT column which provides good ductility to the concrete filled steel tubular columns.

(5) Axial load deformation analysis helps to rectify the mismatched result by considering the previous research in axial deformation of square columns.

5.3 RECOMMENDATIONS

The literature review and analysis procedure utilized in this thesis has provided useful insight for future application of a finite element method for analysis. FEM model helps in comparing the results with experimental results data. Modelling the concrete filled

steel tubular columns in FEM based ATENA software gives approximate results which can be included in future research.

5.4 FUTURE SCOPE

In the present study concrete filled steel tubular columns has been studied under axial loading. Concrete filled steel tubular columns can be studied under cyclic loading and also use reinforcement. Stress and strain analysis of CFST under cyclic loading can be studied. CFST column confined by tie bars can be studied under various loading conditions. Dynamic analysis of CSFT can also be incorporated in the study.

REFERENCES

1. Alani, Y, R, A.; Agarwal, V, C. (2013), "Nonlinear finite element study on circular concrete filled steel tubular columns", international journal of innovative technology and exploring engineering, volume 3, 52-55.

2. ATENA 3D and ATENA WIN – "finite element software manual".

3. ATENA theory manual, part1 from Vladimir Cervenka, Libor Jendele and Jan Cervenka.

4. Bukovska, P. (2012), "Influence of concrete strength on the behaviour of steel tubular columns filled with concrete", international journal of mechanics, volume 6, 149-157.

5. Cervenka, V.; Cervenka, J.; Pukl, R. (2002) "ATENA- a tool for engineering analysis of fracture in concrete", Sadhana, 27.4, 485-492.

6. Chitawadagi, V, M.; Narsimahan, M, C.; Kulkarni, S, M. (2010), "axial strength of circular concrete filled steel tube columns – DOE approach", journal of construction steel research, 66, 1248-1260.

7. Dai, X, H.; Lam, D.; Jamaluddin, N.; Ye, J. (2014), "Numerical analysis of slender elliptical concrete filled columns under axial compression", thin walled structures, 77, 26-35.

8. Dundu, M. (2012), "compressive strength of circular concrete filled steel tube columns", journal of thin walled structures", 56, 62-70.

9. El-Heweity, M, M. (2012), "On the performance of circular concrete filled high strength steel columns under axial loading", Alexandria engineering journal, 51, 109-119.

10. Evirgen, B.; Tuncan, A.; Taskin, K. (2014), "Structural behaviour of concrete filled steel tubular sections under axial compression", thin walled structures, 80, 46-56.

11. Gajalakshmi, P.; Helena, H, J.; Raghavan, R, S. (2011), "Experimental investigation on the behaviour of concrete filled steel tubular columns", Asian journal of civil engineering, volume 12, 691-701.

12. Ghannam, S.; Al-Ani, H, R.; Al-Rawi, O. (2010), "Comparative study of load carrying of steel tube columns filled with light weight concrete and normal concrete", Jordan journal of civil engineering, volume 4, 164-169.

13. Gupta, P, K.; Sarda, S, M; Kumar, M, S. (2007), "Experimental and computational study of concrete filled steel tubular columns under axial loads", journal of constructional steel research, 63, 182-193.

14. Hu, H, T.; Huang, S, C.; Chen, Z, L. (2005), "Finite element analysis of CFT columns subjected to an axial compressive force and bending moment in combination", journal of constructional steel research, 61, 1692-1712.

15. Kvocak, V.; Varga, G.; Vargova, R. (2012), "Composite steel concrete filled steel tubes", Procedia engineering, 40, 62-70.

16. Kwasniewski, L.; Szmigiera, E.; Siennicki, M. (2012), "Finite element modelling of composite concrete steel sections", archives of civil engineering, 4, 373-388.

17. Ma, Y, S.; Wang, Y, F. (2012), "Creep of high strength concrete filled steel tube columns", journal of construction steel research", 53, 91-98.

18. Mahasneh, B, H.; Gharaibeh, E, S. (2005), "Enhancing the filled tube properties by using the fiber polymers in filling matrix", journal of applied sciences, 5, 232-235.

19. Patidar, A, K. (2012), "Behaviour of concrete filled rectangular steel tube column", IOSR journal of mechanical and civil engineering, volume 4, 46-52.

20. Patil, V, P. (2012), "Finite element approach to study the elastic instability of concrete filled steel tubular columns under axial loads", international journal of emerging technology and advanced engineering, volume 2, 276-284.

21. Schneider, S, P. (1998), "Axially loaded concrete filled steel tubes", journal of structural engineering, 1125-1138.

22. Singh, H.; Gupta, P, K. (2013), "Numerical modelling of rectangular concrete filled steel tubular short columns", International journal of scientific and engineering research, volume3, 52-55.

23. Song, T, Y.; Han, L, H.; Yu, H, X. (2010), “concrete filled steel tube stub columns under combined temperature and loading”, journal of construction steel research, 66, 369-384.

24. Tao, Z.; Wang, Z, B.; Yu, Q. (2013), “Finite element modelling of concrete filled steel stub columns under axial compression”, journal of constructional steel research, 89, 121-131.

25. Uy, B.; Tao, Z.; Lizo, F, Y.; Han, L, H. (2009), “Behaviour of slender square concrete filled stainless steel columns to axial loads”, Nordic steel construction conference, 359-366.